Enhanced Biological Activity of Metal Nanoparticles-

(-) Epicatechin Bioconjugate with Protein

By

C.DEVASRI

(20PPH005)

A Thesis submitted to

Avinashilingam Institute for Home Science and Higher Education for Women

Coimbatore-641 043

In partial fulfilment of the requirements for the degree of

MASTER OF SCIENCE IN PHYSICS

MAY 2022

Enhanced Biological Activity of Metal Nanoparticles-

(-) Epicatechin Bioconjugate with Protein

BY

C.DEVASRI

(20PPH005)

A Thesis submitted to

Avinashilingam Institute for Home Science and Higher Education for Women
Coimbatore-641 043

In partial fulfilment of the requirements for the degree of

MASTER OF SCIENCE IN PHYSICS

MAY 2022

CERTIFIED AS A BONAFIDE RESEARCH WORK

27/05/22
Signature of the Head of the Department

27/5/22
Signature of the Supervisor

ACKNOWLEDGEMENT

ACKNOWLEDGEMENT

I owe my sincere thanks to **Lord Almighty** and **My Parents** without whom I would have been nothing and showering their generous blessings upon me in all endeavors

I wish to express my deep sense of reverential gratitude to **Prof.S.P.THYAGARAJAN**, Chancellor, Avinashilingam Institute for Home Science and Higher Education for Women, Coimbatore, for providing the facilities to conduct this study.

I extend my thanks to **HON.Dr.V.BHARATHI HARISHANKAR**, Vice Chancellor, Avinashilingam Institute for Home Science and Higher Education for Women, Coimbatore, for providing flamboyant help towards the completion of the study.

I record my deep sense of gratitude and indebtedness to **Dr.S.KOWSALYA,** Registrar, Avinashilingam Institute for Home Science and Higher Education for Women, Coimbatore, for providing adequate help for the study.

I also wish to express my gratitude to **Dr.(Mrs).G.PADMAVATHI,** Dean, school of physical sciences and computational sciences, Avinashilingam Institute for Home Science and Higher Education for Women, Coimbatore, for timely help rendered throughout the course.

I whole heartily thank **Dr.J.SHANTHI**, Professor and Head of the Department of Physics, Avinashilingam Institute for Home Science and Higher Education for Women, Coimbatore, for her encouragement and generous help which was of great value.

I are very much indebted to my Guide, **Mrs.S.ANITHA**, Assistant Professor, Department of Physics, Avinashilingam Institute for Home Science and Higher Education for Women, Coimbatore, for her excellent, outstanding guidance, constructive criticism, motivation, valuable advice, untiring support, timely suggestions, holding me strong in all the places when we faltered.

I thank **Dr.V.SASIREKHA** and **all the staff members of the Department of Physics**, Avinashilingam Institute for Home Science and Higher Education for Women, Coimbatore, for being supportive and guidance.

I also express my gratitude to **TAMILNADU STATE COUNCIL FOR SCIENCE AND TECHNOLOGY** for Sanctioning student project PS-334 (2021-2022).

I thank all my friends for their support, understanding and co-operation for the successful completion of the study.

DEVASRI C

LIST OF CONTENTS

CONTENTS

LIST OF FIGURES

LIST OF TABLES

INTRODUCTION

CHAPTER I
INTRODUCTION

1.1 Introduction

Proteins are the most abundant molecule found in the living Organisms. The hormones and enzymes which control the metabolism, the framework forming collagen in bones, the contractile proteins in muscles, to the hemoglobin and albumin in the bloodstream and immunoglobulin's fighting infections, almost every life process relies on this class of molecules. Albumin is the most abundant protein in the vertebrates' organisms (up to 40 mg/ml) and the most prominent plasma protein (about 60% of the total protein content of plasma). It is one of the first discovered and most intensely studied proteins [1].The investigation of the binding amplitude and mechanism of interaction of small molecules with serum albumins is crucial for the understanding of drug pharmacodynamics and pharmacokinetics, as the nature and strength of that interaction has a great influence on drug absorption, distribution, metabolism and excretion [2,3]

Serum albumin (SA) is the most abundant plasma protein in mammals. SA is a multifunctional protein with extraordinary ligand binding capacity, making it a transporter molecule for a diverse range of metabolites, drugs, nutrients, metals and other molecules. Due to its ligand binding properties, albumins have wide clinical, pharmaceutical, and biochemical applications.The evaluation of small molecules affinity for albumins, bovine serum albumin (BSA) is usually selected as a relevant model, due to its structural similarity with human serum albumin (76%), its low cost and wide availability.[4]

1.2 Bovine Serum Albumin

Bovine serum albumin (BSA) is a serum albumin protein derived from cows. It is often used as a protein concentration standard in lab experiments. Bovine serum albumin is often used as protein supplement in cell culture media, and residual bovine serum albumin in some formulations has occasionally caused adverse effects. Symptoms are usually mild, such as itching and urticarial. An anaphylactic reaction has been described in a patient undergoing bone marrow transplantation after the bone marrow cells had been kept in bovine serum albumin. The component of sperm processing media, bovine serum albumin has caused adverse effects after intrauterine insemination. Bovine serum albumin has also been reported to cause membranous nephropathy in early childhood.[5]

The BSA molecule consists of 583 amino acids, bound in a single chain cross-linked with 17 cystine residues (eight disulfide bonds and one free thiol group), and has a molecular mass of 66400 Da. The amino acid chain is made up of three homologous but structurally distinct domains (I, II and III), divided into nine loops by the disulfide bonds and arranged in a heart-shaped molecule as shown in the (Fig 1.1). Each domain consists of two sub-domains, A and B. The secondary structure of the protein is mainly α-helical (74%), with the remaining polypeptide chain occurring in turns and in extended or flexible regions between subdomains.[6]

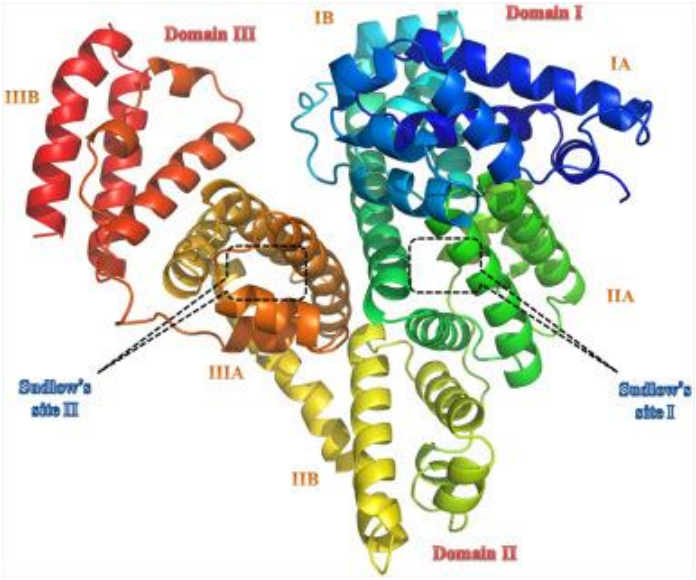

Fig 1.1 Structure of Bovine Serum Albumin

1.2.1 Uses of Bovine Serum Albumin

BSA is used in biochemistry in scientific assays such as the Enzyme-linked Immunosorbent Assay (ELISA).The ELISA is used to detect antibodies or antigens in samples. It is used to diagnose illnesses such as AIDS, malaria or tuberculosis. In immunohistochemistry BSA is used to study hoe cancerous tumors behave and grow. In cell culture, BSA is used in cell culture mediums as a supplement to feed cells and support cell growth. It is an important ingredient in cell sports drinks because it promotes cell growth, healthy and longevity.

BSA caries nutrients to cells and binds free radicals and toxins to reduce cell damage. It also binds hormones and growth factors in order to act as a buffer and keep them stable. BSA is used because of its stability to increase signal in assays, its lack of effect in many biochemical reactions, and its low cost, since large quantities of it can be readily purified from bovine blood, byproduct of the cattle industry.

1.2.2 Properties of Bovine Serum Albumin

Serum albumin are the major native carrier found in the blood and involved in the transporting and delivering of exogenous and endogenous materials (fatty acids, nutrients, steroids, and a variety of therapeutic drug). It must be noted that the effectiveness of drug solubility, bio distribution and their interaction is highly affected by their binding nature and interaction with protein. Strong binding can decrease the concentration of free drugs in plasma where as weak binding may lead to poor distribution and had short life time.[7]

1.3 Amino Acids

Amino acids is a group of organic molecules that consist of a basic amino group (—$_{NH2}$), an acidic carboxyl group (—$_{COOH)}$, and an organic R group (or side chain) that is unique to each amino acid. The term amino acid is short for α-amino [alpha-amino] carboxylic acid. As shown in the Fig 1.2 each molecule contains a central carbon (C) atom, called the α-carbon, to which both an amino and a carboxyl group are attached. The remaining two bonds of the α-carbon atom are generally satisfied by a hydrogen (H) atom and the R group. . Amino acids containing an amino group bonded directly to the α-carbon are referred to as *α-amino acids*.An amino acid is a type of organic acid that contains a carboxyl functional group (-COOH) and an amine functional group (-NH2) as well as a side chain (designated as R) that is specific to the individual amino acid. The elements found in all amino acids are carbon, hydrogen, oxygen, and nitrogen, but their side chains may contain other elements as well. Shorthand notation for amino acids may be either a three-letter abbreviation or a single letter. For example, valine may be indicated by V or val; histidine is H or his .Amino acids may function on their own, but more commonly act as monomers to form larger molecules. Linking a few amino acids together forms peptides, and a chain of many amino acids is called a polypeptide. Polypeptides may be modified and combine to become proteins.[8]

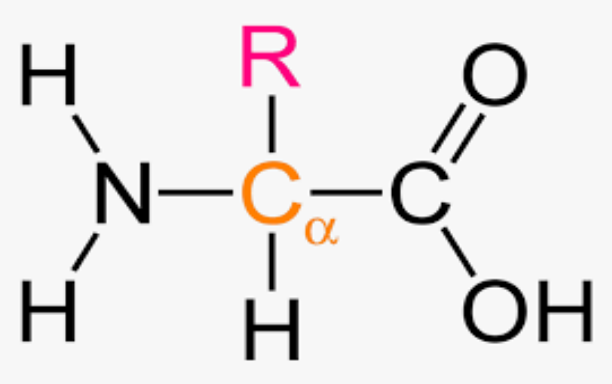

Fig 1.2 – Structure of Amino acid

1.3.1 Functions of Amino Acids

Amino acids are used to build proteins and most of the human body consists of them. Their abundance is second only to water. Amino acids are used to build a variety of molecules and are used in neurotransmitter and lipid transport.[9]

1.4 Polyphenols

Polyphenols are a category of compounds naturally found in plant foods, such as fruits, vegetables, herbs, spices, tea, dark chocolate, and wine. They can act as antioxidants, meaning they can neutralize harmful free radicals that would otherwise damage your cells and increase your risk of conditions like cancer, diabetes, and heart disease. Polyphenols are also thought to reduce inflammation, which is thought to be the root cause of many chronic illnesses.[10]. (Fig1.3) shows the classification of polyphenols.

1.4.1 Types of Polyphenols

- ❖ Flavonoids.
- ❖ Phenolic acids.
- ❖ Polyphenolic amides.
- ❖ Other polyphenols.[11]

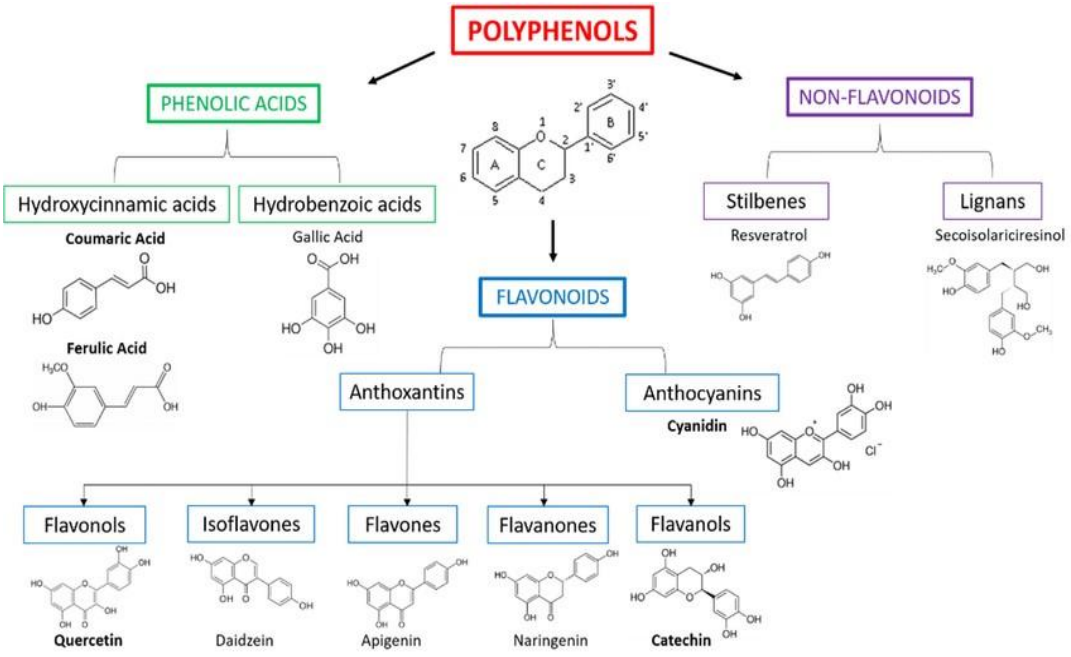

Fig 1.4 Classification of Polyphenols

1.4.2 Bioactivity of Natural Polyphenols

The reactive oxygen species (ROS) play an important role in many diseases, such as cardiovascular diseases, cancer, ageing, neurodegenerative diseases and diabetes. Natural polyphenols are the biggest group of phytochemicals, and have attracted more and more attention as potential agents for prevention and treatment of oxidative stress-related diseases. Natural polyphenols are secondary metabolites of plants, and many of them have been found in plantbased foods. Polyphenols have effects on the bitterness, astringency, colour, flavour, odour and oxidative stability in food. Natural polyphenols have been widely studied, and found to possess many important bioactivities. Special attention has been made to the bioactivities, such as antioxidant, cardio protective, anticancer, anti-ageing, anti-inflammation and antimicrobial properties.

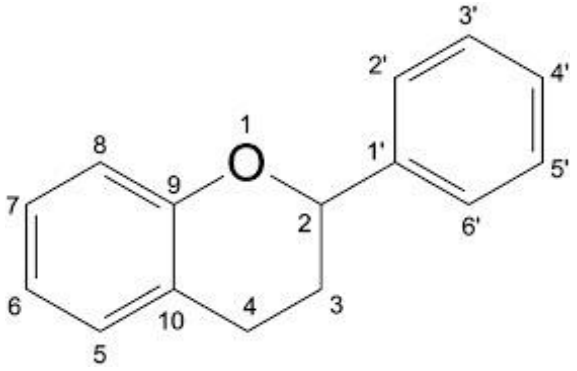

Fig 1.5 Natural Polyphenols

1.4.3 Bioavailability of Polyphenols

Bioavailability is usually defined as the fraction of an ingested nutrient or compound that reaches the systemic circulation and the specific sites where it can exert its biological activity. The conclusive evidence for the effectiveness of dietary polyphenols in disease prevention and human health improvement, it is useful to better define the bioavailability of polyphenols. The health effects of polyphenols in human and in animal models depend on their absorption, distribution, metabolism and elimination. The chemical structure of polyphenols determines their rate and extent of absorption as well as the nature of the metabolites present in the plasma and tissues. The most common polyphenols in human diet are not necessarily the most active within the body,either because they have a lower intrinsic activity or because they are poorly absorbed from the intestine, highly metabolized, or rapidly eliminated.[12]

1.5 Flavonoids:

Flavonoids are a diverse group of phytonutrients (plant chemicals) found in almost all fruits and vegetables. Along with carotenoids, they are responsible for the vivid colors in fruits and vegetables. Flavonoids are the largest group of phytonutrients, with more than 6,000 types.Flavonoids are the most common and widely distributed group of plant phenolic compounds, occurring virtually in all plant parts, particularly the photosynthesizing plant cells. Flavonoids consist of both antioxidant and anti-inflammatory properties, found in fruits, vegetables, legumes, red wine, and green tea. More than 4000 flavonoids have been identified in plants. Some of the best-known flavonoids are quercetin and kaempferol Chemically flavonoids are based upon a fifteen-carbon skeleton consisting of two benzene rings (A and C) linked via a heterocyclic pyrane ring (B) (Fig.1.4). Flavonoids can be divided into 6 subclasses. They are

- Flavonols
- Flavones
- Flavanones
- Isoflavones
- Anthocyanidins,
- Flavanols[13]

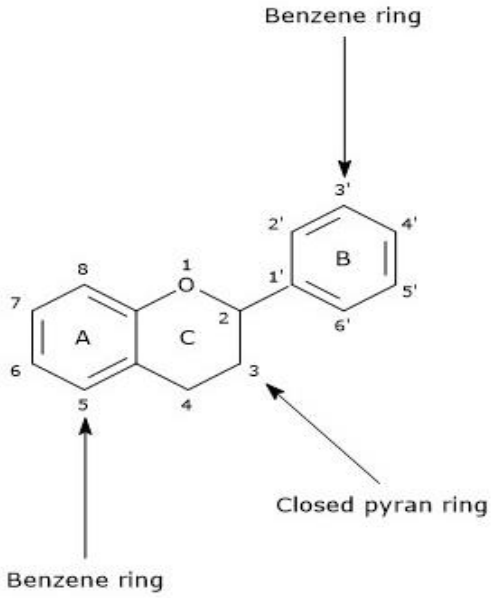

Fig 1.4 Structure of Flavonoids

1.5.1 Biological Functions of Flavonoids

The biological functions of flavonoids are linked to their potential cytotoxicity and their capacity to interact with enzymes through protein complexation. Some flavonoids provide stress protection, for example, acting as scavengers of free radicals such as reactive oxygen species (ROS), as well as chelating metals that generate ROS via the Fenton reaction. Flavonoids are also involved in the resistance to aluminum toxicity in maize. Roots of maize plants that were exposed to aluminum exuded high levels of phenolic compounds such as catechin and quercetin. Indicating their ability of chelating metals can be an *in vivo* mechanism to ameliorate aluminium toxicity. Auxins probably have a role in the stress response by controlling stomatal opening and by allocating resources under poor growth conditions.[14]

1.5.2 Chemical Structure of Flavonoids

The structure of flavonoids is a skeleton of diphenyl propane, with two benzene rings (ring A and B) shown in fig 1.7 linked by a three-carbon chain, which forms a closed pyran ring (heterocyclic ring containing oxygen, the C ring) with benzenic A ring, referred to as C6-C3-C6. In some flavonoids, B ring binds with ring C either in position of 2,3 or 4, which had the pattern of glycosylation and hydroxylation. Flavonoids possess high antioxidant activity and act as scavengers to repair the damaged cells.[15]

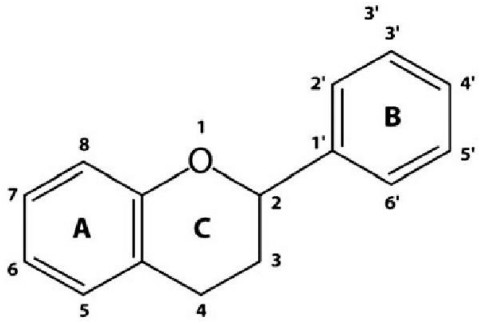

Fig 1.5 Skeleton of Diphenylpropane

1.5.3 Classification of Flavonoids

Flavonoids can be subdivided into different subgroups depending on the carbon of the C ring on which B ring is attached due to degree of unsaturation and oxidation of the C ring. Flavonoids, in which B ring is linked in position 3 of the ring C called isoflavones, B ring is linked in position 4 called neoflavanoids. The B ring is linked in position 2 can be further subdivided into several subgroups are: flavones**,** flavonols**,** flavanones**,** flavanonols**,** flavanols or catechins and anthocyanins. Finally, flavonoids with open C ring called chalcones.

1.5.4 Flavones

Flavones are double bond between positions 2 and 3 and ketone in position 4 of the C ring. Most flavones had hydroxyl group in position 5 of the A ring, while the hydroxylation occurs in position 7 of the A ring or 3′. 4′ of the B ring vary according to the taxonomic classification of the particular vegetable or fruit.

1.5.5 Flavonols

Flavonols had a hydroxyl group in position 3 of the C ring, and are glycosylated, which present in many plants.

1.5.6 Flavanones

Flavanones are dihydroxyflavones in which C ring saturated with double bond between positions 2 and 3. The flavanones are multi-hydroxylated, and many hydroxyl groups can be glycosylated and methylated.

1.5.7 Flavanonols

Flavanonols, also called dihydroflavonols, which are the 3-hydroxy derivatives of flavanones.

1.5.8 Isoflavones

Isoflavones are a subgroup of flavonoids in which the B ring is attached to position 3 of the C ring.

1.5.9 Flavanols/ Flavan-3-Ols/Catechins

Flavanols have two chiral centers on positions 2 and 3 in the molecule and form four possible diastereoisomers. ECT is the isomer with the *cis* configuration and catechin with *trans* configuration. Each of these configurations had two stereoisomers, namely, (+) ECT and (-)-ECT, (+)-catechin and (-)-catechin. (+)-Catechin and (-) ECT are the two isomers present in edible plants. Catechin and ECT had an ability to form polymers, namely proanthocyanidins or condensed tannins. The name proanthocyanidins is due
to the fact that an acid-catalysed cleavage produces anthocyanidins. Proanthocyanidins typically contain 2 to 60 monomers of flavanols. Monomeric and oligomeric flavanols (containing 2 to 7 monomers) are strong antioxidants.

1.5.10 Anthocyanidins

Anthocyanidins are flavylium cations that gives plants colors, while others are colourless. Anthocyanins are glycosides of anthocyanidins. The colour of the anthocyanins depends on the pH.

1.5.11 Chalcones

Chalcones and dihydrochalcones are flavonoids with open structure and have similar synthetic pathways.[16]

1.5.12 Epicatechin (ECT)

(-) ECT is a well-studied polyphenol with respect to the effect noticed in diabetes and obesity, through various mechanisms. (-)ECT is a catechin that is flavan carrying five hydroxy substituents at positions 3, 3', 4', 5 and 7 (the 2S,3S-stereoisomer). The structure of ECT is constituted by resorcinol (A ring) and catechol (B ring) moiety, which is interconnected by a benzopyron ring (C ring) is shown in (Fig.1.6).The molecular formula for ECT is $C_{15}H_{14}O_6$ and molecular weight 290.27. ECT has a role as a cyclooxygenase 1 inhibitor and a plant metabolite. It is a catechin and a polyphenol. ECT reduces the accumulation of final products of glycosylation produced in retina during diabetes. In cancer, ECT both in vivo, as well as in vitro studies, presents a good candidate as antineoplastic or cancer prevention, by inducing apoptosis via mitochondria, changes in the morphology of the nucleus of tumor cells, fragmentation of DNA, and cell arrest among others.[17]

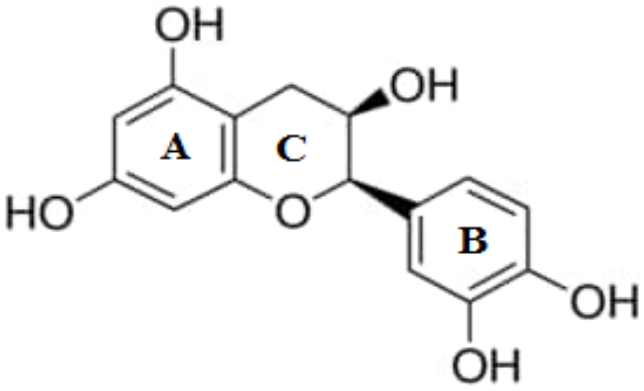

Fig 1.6 Structure of ECT

1.6 Metal Nanoparticle

Metal nanoparticles are submicron scale entities made of pure metals (e.g., gold, platinum, silver, titanium, zinc, cerium, iron, and thallium) or their compounds (e.g., oxides, hydroxides, sulfides, phosphates, fluorides, and chlorides). One of the most documented nanosystems is silver nanoparticles. Due to their small size, they have a large area available for oxidation. Silver nanoparticles, either as dispersion or incorporated into different materials, have shown different properties and applications in dental practice as antimicrobials, caries inhibitors, dental restorative materials, endodontic retrofilling cement, dental implants, and intraoral devices to prevent microbial accumulation (e.g., mouth guards). Gold nanoparticles have also showed high bactericidal activity by a synergistic action with gallic acid. This promising antibacterial effect has attracted considerable interest from researchers and pharmaceutical companies due to their high microbial resistance to antibiotics and the development of resistant.[18]

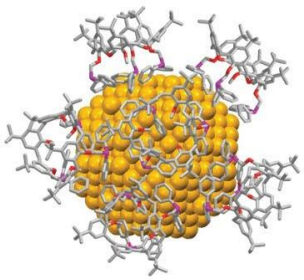

Fig 1.7 Structure of Metal nanoparticle

1.6.1 Silver Nanoparticles

Silver nanoparticles (AgNPs) are nanoparticles of silver of between 1 nm and 100 nm in size. Numerous shapes of nanoparticles can be constructed depending on the application at hand. Commonly used AgNPs are spherical, but diamond, octagonal, and thin sheets are also common. Their extremely large surface area permits the coordination of a vast number of ligands. The properties of AgNPs applicable to human treatments are under investigation in laboratory and animal studies, assessing potential efficacy, biosafety, and bio distribution. AgNPs are increasingly used in various fields, including medical, food, health care, consumer, and industrial purposes, due to their unique physical and chemical properties.

These include optical, electrical, and thermal, high electrical conductivity, and biological properties. Due to their peculiar properties, they have been used for several applications, including as antibacterial agents, in industrial, household, and healthcare-related products, in consumer products, medical device coatings, optical sensors, and cosmetics, in the pharmaceutical industry, the food industry, in diagnostics, orthopedics, drug delivery, as anticancer agents, and have ultimately enhanced the tumor-killing effects of anticancer drugs. AgNPs have been frequently used in many textiles, keyboards, wound dressings, and biomedical devices. Nano sized metallic particles are unique and can considerably change physical, chemical, and biological properties due to their surface-to-volume ratio; therefore, these nanoparticles have been exploited for various purposes.[19]

Fig 1.8 Structure of AgNPs

1.7 Objectives of the Present Work:

- To Synthesize AgNPs using ECT.
- To Interact ECT and bioconjugated ECT +AgNPs with BSA.
- Bioconjugate of ECT and ECT +AgNPs by spectroscopic methods has to be analysed.
- The antibacterial activity of complex BSA-ECT and BSA-ECT-AgNPs on the *Gram positive* and *Gram negative bacteria's* were to be examined.
- Using Molecular Docking Studies, the hydrophobic and hydrogen bonds interactions between the complexes of ECT-BSA and BSA-(ECT-AgNPs) were analysed.

REVIEW OF LITERATURE

CHAPTER II

REVIEW OF LITERATURE

2.1 Introduction

This chapter deals about the reviews on the interaction of metal nanoparticles with protein and flavonoids. Various studies have been listed below which shows a number of characterization methods to analyze the interactions between the complexes.

2.2 Overview of Literature

Junwei Zhao et.al. (2022) synthesized the biocompatible bovine serum albumin (BSA) coated Ag^2S nanoparticles (NPs), at mild temperature for PTT of cancer. The high photo thermal conversion efficiency of the obtained Ag^2S NPs with strong NIR absorption is about 18.89%, which make them ideal materials for photo thermal agents. The Ag^2S NPs can induce effective apoptosis of tumor cells exposed to an NIR laser (808 nm), realizing an effective PTT with excellent killing effect of tumor cells. This work provides a simple reproducible method to fabricate the water-soluble and biocompatible Ag^2S NPs, which would provide new insights of designing new functional NPs for the PTT therapy of tumor[20].

Sourav Das et.al.,(2021) synthesized the AgNPs using green tea (GT) extract and two of its components, (−)-epigallocatechin gallate (EGCG) and (+)-catechin (Ct) as capping/stabilizing agents is reported. The synthesized AgNPs showed antibacterial activity against the bacterial strains Staphylococcus aureus and *Escherichia coli,* along with anticancer activity against HeLa cells. After administering nanoparticles to the body, they come in contact with proteins and results in the formation of a protein corona.This interactions of these biocompatible AgNPs with hen egg white lysozyme (HEWL) as a carrier protein was also studied. Static quenching mechanism was accountable for the quenching of HEWL fluorescence by the AgNPs. The binding constant (K_b) was found to be higher for EGCG-AgNPs ($(2.309 \pm 0.018) \times 10^4\ M^{-1}$) than for GT-AgNPs and Ct-AgNPs towards HEWL. EGCG-AgNPs increased the polarity near the binding site while Ct-AgNPs caused the opposite effect, but GT-AgNPs had no such observable effects. Circular dichroism studies indicated that the AgNPs had no such appreciable impact on the secondary structure of HEWL.The –OH groups of the polyphenols drive the in site capping/stabilization of the AgNPs during synthesis, which might offer new opportunities having implications for Nano medicine and Nano diagnostics[21].

Jules-blaise mabou leuna et.al.,(2021) studied the mechanism of the electrochemical oxidation of (-)-ECT (ECT) in a hydro-alcoholic medium, at a glassy carbon electrode, using cyclic and square wave voltammetric techniques and at different pHs. It proceeds in a cascade mechanism related to the two resorcinol hydroxyl groups and the other three hydroxyl groups in ECT which present electroactivity and is pH-dependent. The oxidation of the 30,40 -dihydroxyl moiety, occurs first at a very low positive potential, and it is a two-electron/ two proton reversible reaction. The proposed mechanism is an ECE type mechanism. After the addition of bovine serum albumin (BSA) to ECT solution, the oxidation peak currents decreased with no peak potential shift and no new peaks appeared. The diffusion coefficients of both free and bound ECT were estimated from the cyclic voltammetry data (Df = 2.37 9 10-10 cm2 s -1 and Db = 6.28 9 10-11 cm2 s -1). An ECT-BSA complex is formed with binding constant Kapp = 1.8 9104, calculated from UV-vis spectroscopy data [22].

Anitha et.al.,(2021) investigated the interaction of two stereo isomeric flavanols (+) catechin (CT) and (−) ECT with bovine serum albumin (BSA)using UV–Vis absorption and fluorescence spectroscopy. The binding affinity between flavanols and BSA is investigated through fluorescence quenching. Fluorescence study shows that both flavanols exhibit a strong interaction with BSA at a single binding site. This investigation indicates that CT/ECT may quench BSA fluorescence by the static quenching process due to the formation of ground state complex. The binding pocket of BSA is identified at the site I/II with the interaction of CT/ECT using molecular docking studies. Molecular dynamics simulation (MDS) reported the structural changes of BSA into sturdy α-helix formations owing to the interaction of CT/ECT. During the 200 ns simulation, BSA-ECT complex had lower root mean square deviation values, and undergoes slight structural deformations. The MDS result shows that the binding of CT/ECT with BSA is due to hydrophobic and hydrogen bond interactions, which supports the experimental outcomes. The analysis of radius of gyration confirmed that the BSA-ECT complex possessed a more compact structure. CT and ECT differ in their binding site and structural effects caused by distinct orientational positions at the benzopyran moiety. These findings helps to understand the binding nature of CT/ECT with BSA protein, and the effect of protein during blood transportation process 23].

Sedigheh Hashemnia et.al.,(2021) investigated the influence of AgNPs on the binding of clonazepam to bovine serum albumin (BSA) using ultraviolet-visible (UV–Vis), fluorescence, and circular dichroism (CD) spectroscopic methods. Detailed insights into the binding sites of clonazepam on the PVP-AgNPs surface in the absence and presence of BSA have been obtained by carrying out molecular dynamics (MD) simulations and molecular docking analysis. UV–Vis results show that the interaction between BSA and AgNPs causes formation of BSA-AgNPs complexes. CD studies imply that the formation of BSA-AgNPs complexes is accompanied by conformational changes in the secondary structural level of the protein. The intrinsic fluorescence of BSA solution in the simultaneous presence of AgNPs and clonazepam shows that clonazepam interacts considerably more with BSA-AgNPs complexes than with BSA. MD simulations results show that clonazepam molecules bind more to the PVP polymer film than to the bare Ag (0) atoms on the PVP-AgNPs surface. Molecular docking analysis shows a binding affinity of −19.77 kJ/mol for BSA-AgNPs complexes. Also, the results show that, although the IIA and IIIA domains in BSA play an important role in the docking of clonazepam with BSA, in BSA-AgNPs complexes, clonazepam molecules bind to the bare $Ag^{(0)}$ atoms, and there is also the possibility of interaction between PVP and BSA via clonazepam.[24].

Daniel J. Boehmler et.al.,(2020) reported the comprehensive analysis of AgNPs dissolution and protein adsorption behaviors with monolayer surface coverage of AgNPs by bovine serum albumin (BSA). AgNPs dissolution rate constants, $k_{dissolution}$, were quantified over several particle sizes (10, 20, and 40 nm) and BSA concentrations (0–2 nM) using linear sweep stripping voltammetry. Across all particle sizes, the dissolution rate constant increased with increasing BSA concentrations. However, protein-enhanced dissolution behaviors were most pronounced for 10 nm AgNPs, which exhibited 3.6-fold and 7.7-fold relative enhancement when compared to 20 and 40 nm AgNPs, respectively. Changes to AgNPs surface properties upon interaction with BSA were monitored using dynamic light scattering and zeta potential measurements, while BSA–AgNPs complex formation was evaluated using UV–vis spectroscopy and circular dichroism spectroscopy. A subtle increase in the BSA–AgNPs association constant was observed with an increase in the AgNPs size. Together, these results suggest that the AgNPs size dependence of BSA-enhanced dissolution of AgNPs is possibly mediated through both displacement of Ag(I)(aq)-loaded BSA by excess protein in the bulk solution and minimized accessibility of the AgNPs surface because of BSA adsorption.[25].

Jie Yang et.al.,(2020) synthesized two mononuclear complexes **[**Co(HL)L**]**NO_3 **(**1**)** and **[**Cu$(HL)_2$**](**NO_3**)**$_2$ **(**2**)** from the reaction of 2-acetylpyridine-4-hydroxy phenylacetyl acylhydrazone (HL) with copper/cobalt nitrate hydrate. The single-crystal XRD results revealed the central Co and Cu ions in two complexes are both six-coordinated showing a distorted octahedral geometry. Thermal stabilities of 1**,** 2 and HL were explored by thermogravimetry (TG) and the apparent activation energy (E_a) followed the order 2 > 1 > HL. The interactions of 1**,** 2**,** HL with calf thymus DNA (CT-DNA) and bovine serum albumin (BSA) were investigated through UV–Vis absorption spectroscopy, fluorescence spectroscopy, microcalorimetry and molecular docking approach. From UV–Vis absorption spectroscopy and fluorescence spectroscopy results, it is shown that 1**,** 2 and HL can bind with CT-DNA by intercalation mode and quench the fluorescence of BSA through static process. The binding constants K_{ib} of three compounds toward CT-DNA/BSA followed the order**:** 1 > 2 > HL**.** Thermogenic curves of three compounds interacting with CT-DNA and BSA were measured by microcalorimetry. The calculated enthalpies, entropies and Gibbs' free energy change ($\Delta H > 0$, $\Delta S > 0$, $\Delta G < 0$) indicated that all the interaction processes were endothermic and spontaneous. Molecular docking results further validated the intercalation binding mode of 1**,** 2 and HL with CT-DNA and the fluorescence quenching of tryptophan in BSA in presence of three compounds. It also demonstrated that hydroxyl, benzene ring, pyridine ring, and carbonyl group of 1**,** 2**,** HL are the most favorable binding site in DNA/BSA interaction. The antimicrobial activities of HL**,** 1 and 2 against *Staphylococcus aureus* (*S. aureus*) and *Bacillus subtilis* (*B. subtilis*) were determined presenting that 1 and HL can inhibit the growth of *S. aureus* and *B. subtilis*, separately. Cellular uptakes of 1 and 2 into *S. aureus* and *B. subtilis* showed the amount of Co accumulation in *S. aureus* is bigger than that of Cu [26].

Md Abrar Siddiquee et.al.,(2019) approached an environment-friendly protocol for the biogenic synthesis of silver nanoparticles (AgNPs) using *Delonix regia* (*D. regia*) leaf aqueous extract as bio-reducing and capping agent. The initial reaction progress was observed by the colour change in the reaction mixture and the AgNPs formation was confirmed by the appearance of surface resonance plasmon (SRP) band at 455 nm by UV–visible spectroscopy. The morphology of the biosynthesized AgNPs was further confirmed by using different techniques such as transmission electron microscopy (TEM), selected area electron diffraction (SAED) and scanning electron microscopy (SEM). The crystalline nature of the biogenic AgNPs was analyzed by X-ray diffraction (XRD) technique. Esterase

like activity of BSA with synthesized AgNPs were investigated. Fluorescence results suggested the contribution of static quenching in the complex formation between AgNPs and BSA. The AgNPs are seen to interact with BSA effectively resulting in structural changes of BSA confirmed by far UV-CD and FT-IR techniques [27].

Junling Wang et.al.,(2019) studied the Bovine Serum Albumin (BSA) is used as the stabilizing reagent for synthesis of silver nanoparticles (Ag-BSA NPs) in aqueous solution, instead of the typical thiol capping agents and unfriendly organic polymers. The optimized preparation formulation of $AgNO_3$:BSA: $NaBH_4$ is at the weight ratio of 1:3.2:0.22, and at least 20g of BSA (4 g Ag NPs +20.0g BSA in one liter volume) is needed to stabilize 4g/L pure silver metal nanoparticle in aqueous solution. The BSA capped silver nanoparticles are extremely stabilized and concentrated in aqueous solution without any aggregation and can even be isolated and stored in solid state. The as-prepared Ag-BSA NPs was fully characterized both in solution and in solid state (UV–Vis, DLS, XRD, SEM (e.g. EDS and EA mapping) and TEM). Their findings can be extended to a wide range of applications of silver nanoparticles in biomedicine and environmental science [28].

Farhat Ikram et,al.,(2018) have examined the ECT capped silver nanoparticles (ECT-AgNPs) as sensor for Pb2+ in blood and water samples. Several metal ions including $Pb^{2+,}$ Ca^{2+}, Ni^{2+}, Cd^{2+}, Zn^{2+}, Co^{2+}, Hg^{2+}, Cu^{2+}, In^{3+}, K^{+}, Li^{+}, Na^{+}, $NH4^{+}$, Cu^{+}, Sn^{2+}, Ba^{2+} and Bi^{3+} were screened. Characterization of ECT-AgNPs-Pb^{2+} complex through AFM showed spherical morphology, particle size measured through DLS was found to be 86.06 nm and Job's plot indicated 1:1binding stoichiometry of this complex. Whereas, ECT-AgNPs can selectively detect Pb^{2+} in a concentration range of 1–100 μM with the detection limit down to 1.52 μM. Variation in pH from 1 to 12 showed that ECT-AgNPs-Pb^{2+} complex is highly stable in basic medium. The synthesized ECT-AgNPs can successfully detect Pb^{2+} in tap water and blood samples[29].

Xiangyu Xu et.al.,(2018) studied the interaction between graphene oxide-sliver nanocomposites (GO-AgNCPs) and bovine serum albumin (BSA) in aqueous buffer solution was investigated by using several spectroscopic and imaging techniques. The visible absorbance intensity of GO-AgNCPs increased with increasing concentrations of BSA, and a slight redshift of the surface plasmon resonance band (SPR) occurred due to the absorption of BSA on the surface of GO-AgNCPs. Fluorescence data revealed a static quenching process of

BSA caused by GO-AgNCPs. Thermodynamic parameters of the absorption process, including adsorption equilibrium constants, changes in Gibbs free energy (ΔG), enthalpy (ΔH) and entropy (ΔS), were evaluated at different temperatures. Negative values of ΔG showed that this process was spontaneous and the BSA-GO-AgNCPs complex might form in aqueous solution. Negative values of ΔH and ΔS suggested that the binding was mainly an enthalpy-driven process, and van der Waals forces and hydrogen bonding were the major force in the formation of the nanoparticle-protein corona. Analysis of synchronous, three dimensional (3D) fluorescence and circular dichroism (CD) spectra demonstrated that the conformation of BSA was slightly altered in the presence of GO-AgNCPs. The protein corona formed on the surface of GO-AgNCPs was directly observed by scanning probe microscopy (SPM)[30].

Farhat Ikram et.al.,(2017) investigated synergistic effect of ECT capped silver nanoparticles (ECT-AgNPs) with gentamicin was investigated in vitro and effect of ECT-AgNPs as a novel type of potential antimicrobial agent with gentamicin was observed. ECT-AgNPs with gentamicin showed remarkable antifungal activity when compared to the antifungal activities of ECT, gentamicin and silver nitrate. Gentamicin when combined with ECT-AgNPs revealed synergistic effect and this combination of ECT-AgNPs with gentamicin enhanced its minimum inhibitory concentration (MIC) value that is, 78.3. When antifungal activity of gentamicin, ECT and silver nitrate was observed then it was noticed that ECT didn't possess antifungal effectiveness, whereas gentamicin and silver nitrate exhibited moderate antifungal effectiveness (MIC =37.9) and (MIC =35.4).ECT-AgNPs induced antifungal effectiveness when combined with gentamicin.[31]

Farhat Ikram et,al.,(2017) found that ECT was used as a coating agent to synthesize ECT coated silver nanoparticles (ECT-AgNPs).Conjugation between ECT and silver was observed through UV–vis and FTIR spectroscopy, whereas particle size and morphology examined by Dynamic light scattering (DLS), atomic force microscopy (AFM) and Scanning electron microscopy (SEM). Stability of ECT-AgNPs was not effected by variation in pH, salt concentration and elevated temperature. Thirty different antimicrobial drugs were mixed and only gentamicin quench absorbance intensity of ECT-AgNPs in the pH range of 1–12 without any noticeable interference. Quenching in the observed concentration range from 0 μM to 100 μM followed Beer's law. Limit of detection and limit of quantification were

found to be 1.28 μM and 4.28 μM respectively. The synthesized ECT-AgNPs exhibited remarkable selectivity for gentamicin in tap water, blood plasma and serum[32].

Jang Hoon Kim et,al.,(2017) examined the (−)-ECT-3,5-*O*-digallate (ECDG) from *Orostachys japonicus* A. Berger for inhibitory activity on α-glucosidase. The results showed that the IC_{50} value was achieved with nanomolar concentrations. Through the enzyme kinetic analysis, ECDG was shown to act as a competitive inhibitor of α-glucosidase by binding to the receptor active site. Fluorescence-quenching measurements showed that ECDG and the enzyme may have a one-to-one reaction with low quenching (K_{sv}) and binding constants. A molecular docking study was performed to evaluate the receptor-ligand complex. Asn236 was found to be particularly important for hydrogen bond formation during the molecular dynamics simulation.[33]

Gebregeorgis A et.al., (2014) elucidated the structure of protein conjugated silver nanoparticles prepared by chemical reduction of $AgNO_3$ and bovine serum albumin (BSA) mixture. The role of BSA in the formation of Ag/BSA nanoparticles was established by UV–Vis Spectroscopy. The association of silver with BSA in Ag/BSA nanoparticles was studied by the decrease in the intensity of absorbance peak at 278 nm in UV–Vis spectra and shift in cathodic peak potential in cyclic voltammogram. The molar ratio of silver to BSA in the Ag/BSA nanoparticles is 27:1, as ascertained by thermogravimetric analysis and atomic absorption spectrometry. Based on atomic force microscopy, dynamic light scattering and TEM(TEM) measurements, the average particle size of nanoparticles was found to be range of 11–15 nm. TEM image showed that the nanoparticle has two distinct phases and selected area electron diffraction pattern of nanoparticles indicated that the silver phase in Ag/BSA is fcc. X-ray photo electron spectroscopy measurements of freshly prepared and argon sputtered nanoparticles provided evidence that the outer and inner region of nanoparticles are mainly composed of BSA and silver respectively. The structural and compositional findings of nanoparticles could have a strong bearing on the bioavailability and antimicrobial activity of nanoparticles.[34]

Zhai Min et.al., (2014) have studied the interaction between BSA and ECT using fluorescence quenching titrations combined with trilinear decomposition method and excitation-emission matrix (EEM) fluorescence. The resolved spectra were highly similar with the actual ones which indicated that the resolved results were reliable.The relevant parameters of the binding process were obtained by quantifying each substance in the

complicated mixtures in site. The quenching was static quenching, ECT had a weak interaction with BSA and the binding site was one. The total concentration and the free concentration of quenchers had different effect on the system. Their results demonstrated that the method exploit in their article is a useful tool to investigate complicated interactions, avoiding complicated pretreatment and simplify experimental procedure[35].

Thomas V et.al., (2013) synthesised Colloidal silver nanoparticles using sol–gel method and these nanoparticles were stabilised by encapsulated into the scaffolds of bovine serum albumin. Silver nanoparticles and encapsulated products were characterised by FTIR, NMR, XRD, TG, SEM and TEM analyses. Silver nanoparticle encapsulated bovine serum albumin showed highly potent antibacterial activity towards the bacterial strains such as *Staphylococcus aureus*, *Serratia marcescens*, *Pseudomonas aeruginosa*, *Escherichia coli* and *Klebsiella pneumoniae*[36].

Goutam Kumar Chandra et.al.,(2012) investigated the interaction of lysozyme (Lyz)-conjugated silver (Ag) nanoparticles with (-)-epigallocatechin gallate (EGCG), one of the major components of green tea. Interaction of a protein with ligand/drug molecules perturbs the conformation of secondary and tertiary structures of the protein.The conformational changes in the tertiary structures of the Lyz molecules on EGCG binding using surface-enhanced Raman scattering (SERS) and circular dichroism (CD) spectroscopic measurements were demonstrated. From the analysis of the amide I band of Lyz in SERS and CD spectra, the site of interaction of EGCG with protein molecules in Lyz-conjugated Ag particles has been identified. Spectroscopic evidence for the conformational response of Trp62 and Trp63, in the β-domain of the protein, to the binding of EGCG has been discussed[37].

Mihaela Skrt et.al.,(2012) reported that polyphenols are responsible for the major organoleptic characteristics of plant-derived foods and beverages.The binding of several polyphenols to bovine serum albumin (BSA) at pH 7.5 and 25 °C: catechins [(−)-epigallocatechin-3-gallate, (−)-epigallocatechin, (−)-ECT-3-gallate, flavones (kaempferol, kaempferol-3-glucoside, quercetin, naringenin) and hydroxycinnamic acids (rosmarinic acid, caffeic acid, p-coumaric acid)were investigated. Fluorescence emission spectrometry and molecular docking were applied to compare experimentally determined binding parameters with molecular modelling. Among these polyphenols, (−)-ECT-3-gallate showed the highest

Stern–Volmer modified quenching constant, followed by (−)-epigallocatechin-3-gallate. Similarly, (−)-ECT-3-gallate had the highest effect on the Circular Dichroic spectrum of BSA, while the changes induced by other polyphenols were negligible. Molecular docking predicted high binding energies for (−)-ECT-3-gallate and (−)-epigallocatechin-3-gallate for the binding site on BSA near Trp213. The above data reveal that the polyphenol structures significantly affect the binding process: the binding affinity generally decreases with glycosylation and reduced numbers of hydroxyl groups on the second aromatic ring[38].

Richard A. Frazier et.al.,(2006) studied the interaction of ECT with bovine serum albumin (BSA)by isothermal titration calorimetry. The binding constant (*K*) and associated thermodynamic binding parameters (*n*, Δ*H*) were determined for the interaction at three solution concentrations of BSA using a binding model assuming independent binding sites. These data show weak non-covalent binding of ECT to BSA. The interaction energetics varied with BSA concentration in the calorimeter cell, suggesting that the binding of ECT induced BSA aggregation. The free energy (Δ*G*) remained constant within a range of 2 kJ mol^{-1} and negative entropy was observed, indicating an enthalpy driven exothermic interaction. It is concluded that the non-covalent ECT–BSA complex is formed by hydrogen bonding.[39]

METHODOLOGY

CHAPTER 3

METHODOLOGY

3.1 Introduction

The protein-bound drugs are projected as next-generation medicines, and therefore the protein-ligand interaction is extensively studied for the designing of drug delivery agent. Proteins are used to protect and transport highly labile cytotoxic chromospheres that react with DNA and lead to strand cleavage. On the other hand, interactions of proteins with drugs can also reduce drug activity. The binding specificity and ability to release a drug is guided by specific encapsulation of drugs in the 3D pockets of protein structures. The binding of geometrical isomers to proteins is of great interest, and the study of such binding would enable one to understand the role of a protein in drug delivery.[40]

This chapter provides a detailed information about the methods and materials which were involved in the enhanced biological activity of metal nanoparticles with the bioconjugate of flavonoids and Protein. This chapter also shows the characterization methods such as UV-Vis spectroscopy, Transmission Electron Microscopy, Fluorescence Spectroscopy, Antibacterial activity and Molecular Docking studies to examine the presence and interaction of the complexes.

3.2 Materials and Methods

3.2.1 Chemicals Used

Table 3.1 List of chemicals used in the experimental work

S.No	Chemicals Used	Chemical formula	Make
1.	Bovine Serum Albumin		Sigma Aldrich
2.	(-) Epicatechin	$C_{15}H_{14}O_6$	Sigma Aldrich
3.	Silver Nitrate	$AgNO_3$	Hi-media

3.2.2 Stock Solution

BSA stock solution (4×10^{-4}M) is prepared in Tris-HCL-NaCl buffer solution (pH=7.4). BSA is dissolved in buffer in order to yield a solution with a concentration of 7×10^{-7}M for spectroscopic measurements. ECT and $AgNO_3$ stock solution is prepared in deionized water with a concentration of 0.17mM.

3.2.3 Synthesis OF AgNPs

The synthesis of AgNPs is carried out by using silver nitrate ($AgNO_3$) solution. 5ml of AgNO3 (0.6mM) and 5ml of ECT (1mM) is dissolved in 20ml of distilled water in the typical synthesis process. The solution is stirred at 80 °C for 45 min under incubation. The formation of AgNPs is observed by the color change.The change of pale yellow color from the bright white color is observed. This color change indicates the formation of AgNPs. (Fig 3.1) shows the color change due to the formation of AgNPs.

Fig 3.1 Synthesis of AgNps. (A) Pure ECT and (B) ECT+AgNps.

3.3 Characterization Techniques

3.3.1 Optical Analysis

3.3.1.1 UltraViolet–Visible (UV–Vis) Spectroscopy

UV-Vis spectroscopy is the measurement and interpretation of electromagnetic radiation absorbed or emitted when the molecules or atoms or ions of a sample move from one energy state to another energy state. UV-Vis spectroscopy is a type of absorption spectroscopy in which light of the ultra-violet region (200-400 nm) is absorbed by the molecule which results in the excitation of the electrons from the ground state to a higher energy state.

Principle of UV-Vis spectroscopy

Basically, spectroscopy is related to the interaction of light with matter. As light is absorbed by matter, the result is an increase in the energy content of the atoms or molecules. When ultraviolet radiations are absorbed, this results in the excitation of the electrons from the ground state towards a higher energy state. The more easily excited the electrons, the longer the wavelength of light they can absorb. The absorption of ultraviolet light by a

chemical compound will produce a distinct spectrum that aids in the identification of the compound.

Light source

Tungsten filament lamps and Hydrogen-Deuterium lamps are the most widely used and suitable light sources as they cover the whole UV region. Tungsten filament lamps are rich in red radiations; more specifically they emit the radiations of 375 nm, while the intensity of Hydrogen-Deuterium lamps falls below 375 nm.

Monochromator

Monochromators generally are composed of prisms and slits. Most of the spectrophotometers are double beam spectrophotometers. The radiation emitted from the primary source is dispersed with the help of rotating prisms. The various wavelengths of the light source which are separated by the prism are then selected by the slits such the rotation of the prism results in a series of continuously increasing wavelengths to pass through the slits for recording purposes. The beam selected by the slit is monochromatic and further divided into two beams with the help of another prism as shown in the (Fig3.2)

Sample and reference cells

One of the two divided beams is passed through the sample solution and the second beam is passé through the reference solution. Both sample and reference solution is contained in the cells. These cells are made of either silica or quartz. Glass can't be used for the cells as it also absorbs light in the UV region.

Detector

Generally, two photocells serve the purpose of the detector in UV spectroscopy. One of the photocells receives the beam from the sample cell and the second detector receives the beam from the reference. The intensity of the radiation from the reference cell is stronger than the beam of the sample cell. This results in the generation of pulsating or alternating currents in the photocells.

Amplifier

The alternating current generated in the photocells is transferred to the amplifier. The amplifier is coupled to a small servometer. The current generated in the photocells is of very low intensity, the main purpose of the amplifier is to amplify the signals many times so we can get clear and recordable signals.

Recording devices

The Time amplifier is coupled to a pen recorder which is connected to the computer. The computer stores all the data generated and produces the spectrum of the desired compound.[41]

The visual and calorimetric appearance of samples were checked by UV–Visible spectrophotometer before and after formulation of AgNPs at different time intervals to ascertain either AgNPs are developed or not. Electronic absorption spectra were recorded using UV–Visible absorption spectrophotometer (V-670-Jasco) in the range of 200–800 nm. Distilled water was used as blank solution.

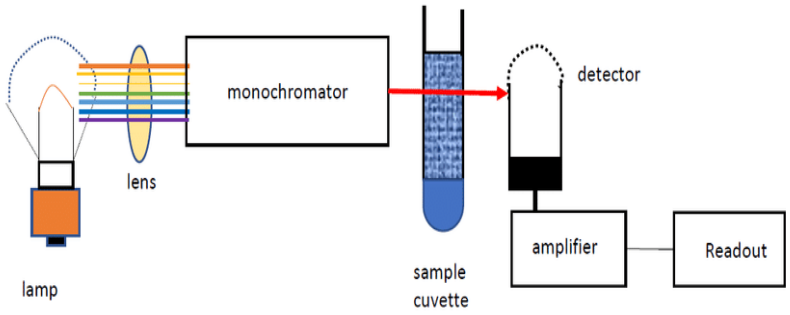

Fig 3.2- A Simplified Schematic of the Main Components in a UV-Vis Spectrophotometer.

Fig 3.3 Ultraviolet–Visible (UV–Vis) Spectrometer.

3.3.1.2 Photoluminescence Spectroscopy

Photoluminescence is a process in which a substance absorbs photons and then re-emits photons. Photoluminescence spectroscopy analyzes the distribution of energies involved in the photo absorption and photoemission processes, the efficiency of the photoemission as well as their temporal characteristics. Because of the non-destructive and contactless nature, photoluminescence spectroscopy applies to solids, solution, solid suspensions, and gaseous materials, making it a highly versatile and sensitive technique for molecular detection and structural analysis.

Photoluminescence (PL) is the spontaneous emission of light from a material following optical excitation. It is a powerful technique to probe discrete energy levels and to extract valuable information about semiconductor sample composition, quantum well thickness or quantum dot sample monodispersity. An electron that has been excited above the conduction band of a material will eventually fall and recombine to the hole that has been excited below the valance band after losing some energy through releasing a phonon to the lowest available non-radioactive energy level. The efficiency of photoluminescence signal is determined by the the nature of optical excitation, properties of material; i.e. radioactive and nonradioactive recontamination and defects.[42].

Pl Instrumentation

A laser tuned to a wavelength close to the bandgap energy of the sample is directed onto the sample. This may be held in a cryostat to facilitate measurements being taken at low temperatures. A rapidly pulsing laser can be used as a quasi constant beam laser since measurements are taken continuously. When the laser beam is incident on the sample, photoluminescence occurs and light is emitted from the sample at wavelengths dependent on the sample composition. The emitted light is directed into a fiber optic cable and then into a spectrometer as shown in the (Fig3.4). A filter may be placed in front of the fiber input to remove any incident laser light. Inside the spectrometer, a diffraction grating diffracts different wavelengths in different directions towards an array of photo-detectors that measure the intensity of each wavelength component. The digital information is interpreted by the computer, which can display a PL spectrum. The spectrum indicates the relative intensities of light of different wavelengths entering the detector.[43]

An RF-5301PC spectrofluorimeter (Shimadzu) equipped with a 150 W Xenon lamp is used for the Fluorescence emission measurements. The fluorescence spectra were recorded with excitation wavelength at 278 nm and 3 nm/3 nm slit widths.To determine the linear concentration range for protein fluorescence, a series of BSA solutions with increasing concentrations (0-25 *i*M) were prepared in buffer. The maximum excitation wavelength (*ì*ex) and maximum emission wavelength (*ì*em) for BSA were 278 and 339 nm, respectively. Therefore, 7×10^{-7} M BSA was chosen as the concentration for fluorescence quenching experiments. For each data point, 2 µL of the appropriate flavonoid solution (Pure ECT, ECT-AgNPs, ECT Buffer) was added into 3 mL BSA solution, a final flavonoid

concentration. The change in fluorescence emission intensity was measured within 1 min of adding flavonoid to the BSA.

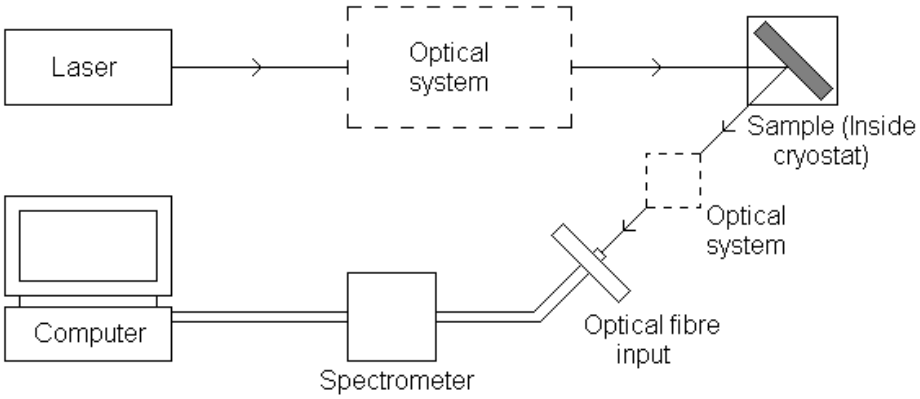

Fig 3.4 Experimental Setup Of Photoluminescence Spectroscopy.

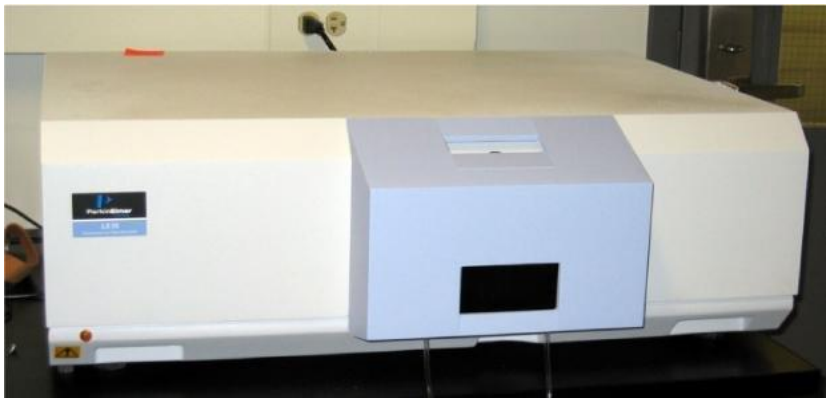

Fig 3.5 Photoluminescence Spectrometer.

3.3.2 Morphological Analysis

3.3.2.1 Transmission Electron Microscopy Analysis.

The TEM is a very powerful tool for material science. A high energy beam of electrons is shone through a very thin sample, and the interactions between the electrons and the atoms can be used to observe features such as the crystal structure and features in the structure like dislocations and grain boundaries. Chemical analysis can also be performed. TEM can be used to study the growth of layers, their composition and defects in semiconductors. High resolution can be used to analyze the quality, shape, size and density of quantum wells, wires and dots. The TEM operates on the same basic principles as the light microscope but uses electrons instead of light. Because the wavelength of electrons is much smaller than that of light, the optimal resolution attainable for TEM images is many orders of magnitude better than that from a light microscope.

Imaging

The beam of electrons from the electron gun is focused into a small, thin, coherent beam by the use of the condenser lens. This beam is restricted by the condenser aperture, which excludes high angle electrons. The beam then strikes the specimen and parts of it are transmitted depending upon the thickness and electron transparency of the specimen. This transmitted portion is focused by the objective lens into an image on phosphor screen or charge coupled device (CCD) camera. Optional objective apertures can be used to enhance the contrast by blocking out high-angle diffracted electrons. The image then passed down the column through the intermediate and projector lenses, is enlarged all the way. The image strikes the phosphor screen and light is generated, allowing the user to see the image. The darker areas of the image represent those areas of the sample that fewer electrons are transmitted through while the lighter areas of the image represent those areas of the sample that more electrons were transmitted through.

Diffraction

Figure 3.6 shows a simple sketch of the path of a beam of electrons in a TEM from just above the specimen and down the column to the phosphor screen. As the electrons pass through the sample, they are scattered by the electrostatic potential set up by the constituent elements in the specimen. After passing through the specimen they pass through the electromagnetic objective lens which focuses all the electrons scattered from one point of the specimen into one point in the image plane. [44]

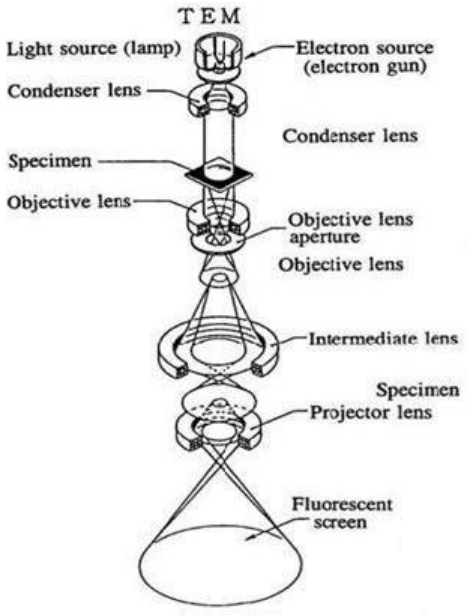

Fig 3.6 TEM

The morphology and size of synthesized silver nanoparticles were examined using transmission electron microscopy. Morphology is analyzed using high resolution transmission electron microscopy (HRTEM, FEI-TECNAI T20 G2).

3.4. Antibacterial Activity

AgNPs are well-known to exhibit a strong antimicrobial activity against various microorganisms such as bacteria, viruses, and fungi due to its smaller in size and large surface area. AgNPs are also widely used as anti-fung, anti-inflammatory, and anti-viral properties. Silver (Ag) has been known to have a toxicity effect over an extensive variety of small organisms, hence silver-based combinations have been widely exploited for its antibacterial applications[45].Antimicrobial susceptibility testing can be used for drug discovery, epidemiology and prediction of therapeutic outcome.Agar plates are inoculated with a standardized inoculum of the test microorganism. Then, the solutions were poured into the well drilled in the petridish containing Agar surface.The Petri dishes are incubated under suitable conditions. Generally, antimicrobial agent diffuses into the agar and inhibits germination and growth of the test microorganism and then the diameters of inhibition growth zones are measured.[46]The antibacterial activity of pure BSA, ECT and bioconjugation of ECT-AgNPs with BSA, is performed by Agar well diffusion method using Muller-Hinton Agar as growth media. The bacterial strains namely *Staphylococcus aureus* (Gram-Positive) and *Pseudomonas aeruginosa* (Gram-Negative) are used in this study. Sterile agar plates were inoculated and 30µl of pure ECT, bioconjugates BSA-ECT, BSA-ECT-AgNPs, ECT-AgNPs were added separately into the wells bored in the agar medium. Then the plates were incubated at 37ºC for 24hrs. A well loaded with antibiotic, Ciprofloxacin served as positive control and was maintained on each plate.

3.5 Theorectical Methods

3.5.1 Molecular Docking

The monomer BSA crystal structure was taken from the Protein Databank (PDB ID:3V03), and the flavanols ECT is used for molecular docking studies. Using the DelWaterObj and DelMol tools, the protein is pre-processed by eliminating the water molecules and co-crystallized flavanols from the coordinate system. The polar hydrogen atoms were then added to the preprocessed protein according to fundamental chemistry principles and the bond sequences were altered using the AddHyd command. Almost 10 independent docking runs were performed, and minimum energy conformers were saved for each complex. AutoDock Vina performed the computation of grid maps and grouping of

dock results automatically. After this complex is formed it is then docked with AgNPs under the same procedure mentioned above. Their Binding affinity is determined using Autodock Vina. LigPlot^{+} is applied to find the configuration of hydrophobic interaction of the amino acid residues of BSA with ECT and BSA with ECT-AgNPs.

3.4.2 Database And Software

Database

PubChem, RCSB Protein Data Bank,The Materials project.

Software

- AutoDock Tools,
- AutoDock Vina,
- Pymol,
- Discovery studio 2017R2,
- The materials project.

Were used for molecular docking. Three main important parts involved in this research. The first part includes the preparation of target protein and ligands, the second is to run the molecular docking stimulation, and the last part is data analysis.[23]

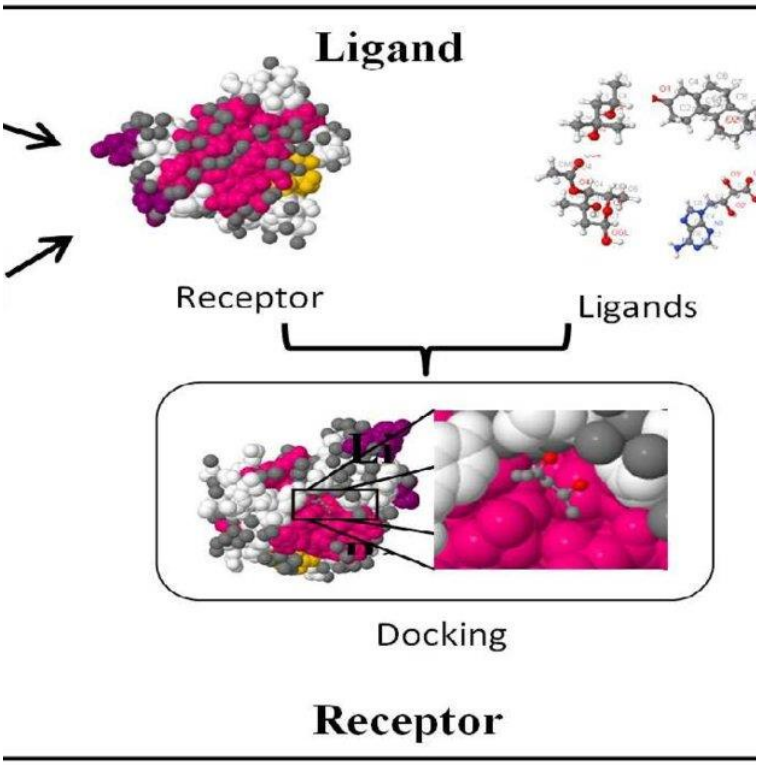

Fig 3.7 Simple model of protein-ligand complex

RESULTS AND DISCUSSION

CHAPTER 4
RESULTS AND DISCUSSION

4.1 Introduction

Metallic nanoparticles show various applications in medicine, biotechnology, and electronics. Silver nanoparticles in particular have attracted attention as antimicrobials, therapeutics and for biomolecular detection, and catalysis. Synthesis methods involving biomolecules are regarded as mild, simple and environmentally friendly.$AgNO_3$ is the most often used precursor for these chemical methods of AgNPs synthesis due to its low cost and high stability.[47]

BSA is taken as a protein and interacted with ECT and ECT-AgNPs. This study helps us to understand the interaction of ECT and ECT-AgNPs with BSA. Their binding characterization have been determined by using UV-Vis spectroscopy. The static quenching mechanism of the complex is analyzed by using Fluorescence Spectroscopy. Their structural characterization is determined through Tem analysis. The binding pockets of the ECT-AgNPs and ECT with BSA were identified using Molecular docking studies. The presence of hydrogen bonds and the hydrophobic bonds were also studied using the Molecular docking method.

4.2 Analysis and Formation of Silver Nanoparticles

4.2.1 UV-Vis Spectral Analysis of AgNPs with ECT

UV-Vis Spectroscopy was used to do Preliminary characterization of the AgNPs. To assess the stability of silver nanoparticles, UV-Vis Spectroscopy was used to examine the generated AgNPs during a 10-day period. The absorption maxima at 395nm indicates the bioreduction ability of ECT from Ag^+ to Ag^0. The UV-Vis spectrum of bioconjugates show a peak at 278 nm, which can be attributed to the presence of pure ECT molecules.The silver nanoparticles exhibited the same peak at the same wavelength with the same absorption intensity even after 10 days as seen in Fig 4.1. The colloidal mixture was found to be stable for 10 days, which was very helpful and convenient for nanoparticle manufacturing.[48]

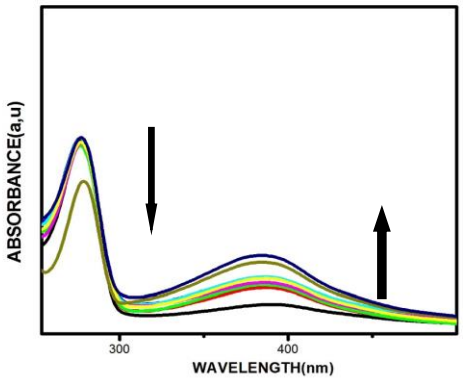

Fig 4.1 UV-Vis absorption spectra of AgNPs synthesized by using ECT

4.2.2 Transmission Electron Microscopy Analysis

Transmission electron microscopy analysis was carried out for the determination of morphology, size of the synthesized AgNPs. Fig 4.2 shows TEM images of the synthesized AgNPs by ECT. The TEM image and size distributions of Ag-NPs showed that the mean diameter of the AgNPs ranged from about 20 to 60 nm. TEM analysis indicated that the synthesized AgNPs using ECT extract were observed to be uniform and mostly spherical in shape. ECT significant role in the reduction of Ag^{+} ions, as stabilizing or capping agents in the synthesis of AgNPs, and may therefore have an effect on the morphology of biocompatible AgNPs. The selected area of electron diffraction pattern indicated that the AgNPs are crystalline in nature, and the bright circular rings signify the presence of different AgNPs planes as shown in the Fig(4.2 c)[49]

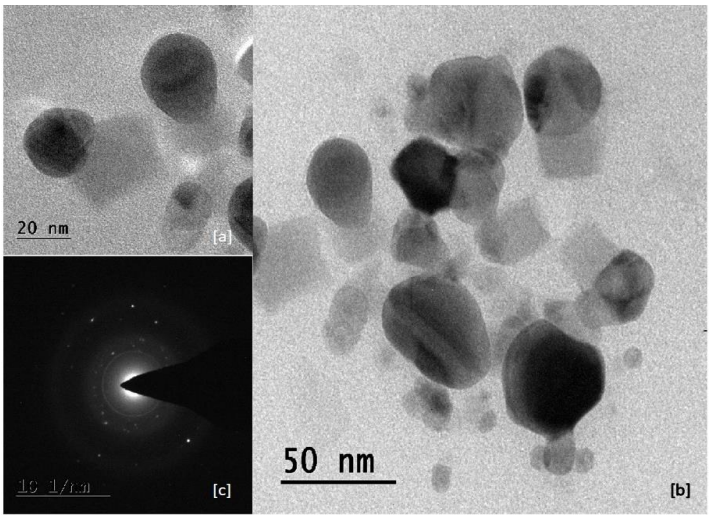

Fig 4.2 TEM image (a) 20nm (b) 50nm and (c) SAED pattern of ECT+AgNPs

4.3 Interaction of ECT and ECT-AgNPs with BSA

4.3.1 UV-Vis absorption spectral analysis of ECT and ECT-AgNPs With BSA

UV-Vis absorption spectral studies are used to examine the formation and conformational fluctuations of BSA protein interacted ECT complexes. The UV-Vis absorption spectra of the complexes BSA-ECT was shown in the Fig 4.3(a).The concentration of BSA in buffer is fixed at 7×10^{-7}M. The ECT (0.17m) of 2µl is titrated step by step into BSA, hence the concentration varies from 1.4×10^{-7}M to 1.4×10^{-6}M. The total accumulated volume of titrated antioxidant solution is 20µl [50]. Two characteristic absorption peaks in the region of 200 to 300nm is absorbed in the UV-Vis absorption spectrum of BSA; one strong absorption peak at 203nm is due to BSA framework, while another absorption maxima appearing at 280nm may be due to *tryptophan,* tyrosine and phenylalanine amino acids.The optical absorbance at 280nm and 203nm increases with increasing the concentration of ECT in BSA.

UV-Vis absorption spectroscopy is the most reliable technique for the study of protein interaction with metal nanoparticles.To examine the impact of bioconjugation on the absorption spectra of BSA and ECT-AgNPs, the UV-Vis absorption spectra of native BSA at various concentrations of ECT-AgNPs were taken and obtained the absorption spectra are shown in Fig. 4.3 b. The concentration of BSA in buffer is fixed at 7×10^{-7}M. The ECT-AgNPs of 2µl is titrated step by step into BSA so that the concentration varies from 1.4×10^{-7}M to 1.4×10^{-6}M. The total accumulated volume of titrated antioxidant solution is 20µl. The absorption spectra of the native form of BSA show an absorption band at 202 nm which arises due to BSA frame while another absorption maxima observed at 278 nm is due to the presence of aromatic amino acid residues (tryptophan and tyrosine) and disulfide bond. It is observed that the absorbance increases regularly on increasing the concentration of ECT-AgNPs[23]. The results obtained from the absorption spectra revealed the complex formation between BSA and ECT-AgNPs.With the increasing concentration of ECT-AgNPs, there is a gradual increase in absorption intensity, indicating the complex formation between the BSA and ECT-AgNPs. This shows that hydrophobic interactions playing a crucial role in the bio-conjugation of ECT-AgNPs with BSA. The results obtained from UV-Vis spectral investigation are in good agreement with the reported literatures about the conjugation of protein with nanoparticles [51]

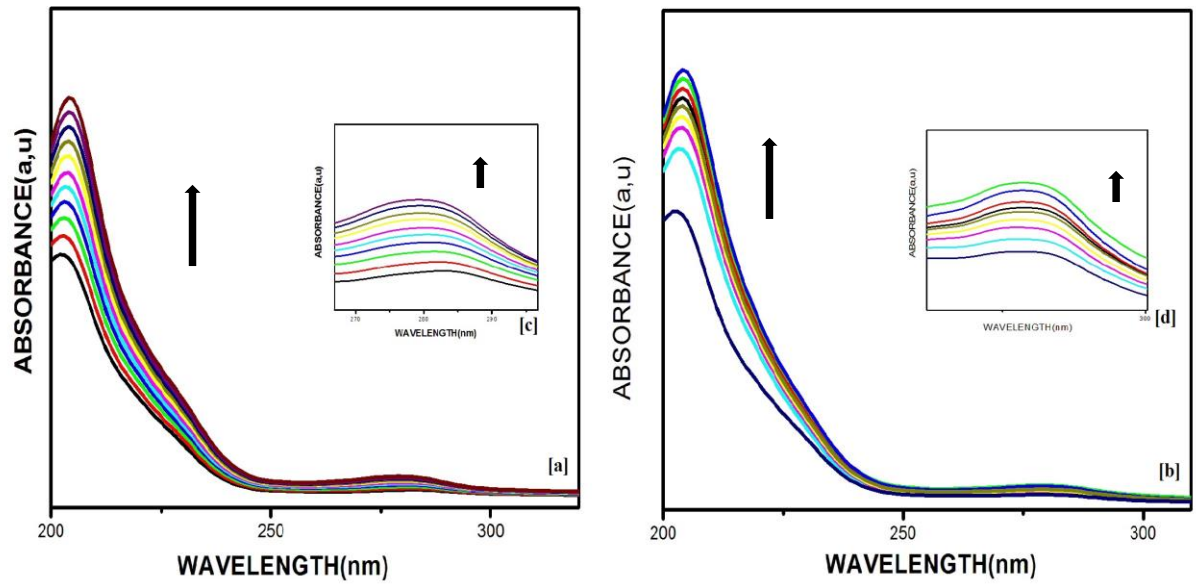

Fig 4.3. UV–Vis absorption spectra of BSA (7x 10^{-7}M) with (a) ECT and (b) ECT-AgNps varies from 0, 1.4×10^{-7} M to 1.4× 10^{-6} M (inset c, d enlarged region from 250 nm to 300 nm).

4.3.2. Fluorescence Quenching of BSA By ECT And ECT-AgNPs

The interaction of ECT and ECT-AgNPs complex with BSA was also monitored by studying the quenching fluorescence of BSA with increasing concentration of BSA. Fluorescence emission spectral analysis was performed to check the effect of ECT-AgNPs and ECT on the fluorescence emission intensity of BSA. The fluorescence quenching spectra of BSA in the presence of the varying concentration of ECT and ECT-AgNPs are shown in Fig. 4.4 a and b. The fluorescence spectrum of BSA is found to have emission maximum at 353 nm with an excitation wavelength of 278 nm, which is mainly attributed to emission of *tryptophan*, tyrosine and phenylalanine residues as shown in Fig 4.4 (a). It is seen that fluorescence intensity of BSA decreases with increase in the concentration of ECT. The progressive quenching in fluorescence intensity shows the formation of a complex between BSA and ECT. It indicates that the ECT can interact with BSA and quench the intrinsic fluorescence of BSA. The result suggests that the fluorophores of BSA is quenched with the possibility of hydrophobic and electrostatic interactions. The hydrophobic interaction may arises due to the changes in the microenvironment of the BSA residues.

The fluorescence spectrum of BSA–ECT-AgNPs is found to have emission maximum at 360 nm with an excitation wavelength of 278 nm. A blue shift of 2nm in fluorescence emission of BSA was seen with an increasing concentration of ECT-AgNPs which is shown in Fig 4.2b. The blue shift showed that the increase in hydrophilicity and polarity around the

fluorophore regions. The fluorescence quenching may be categorized into dynamics and static mechanisms; the former involves the collision between fluorophore and quencher in the excited state of fluorophore while the latter is an outcome of the ground state fluorophore-quencher complex formation

$$F_0/F = 1 + K_{sv}[Q] \quad (1)$$

The Stern-Volmer quenching constant (*Ksv*) and different parameters of the quenching mechanism were calculated by the following equation .Where F_0 and F are the fluorescence intensities of quencher in the absence and presence of quencher respectively, *Ksv* is the Stern-Volmer constant, [Q] is the concentration of quencher, Kq is the quenching rate constant and *τo* is the average fluorescence lifetime of protein fluorophores in the absence of a quencher. Fig.4.5 represents the Stern-Volmer plot, between F_0/F versus [Q] . The obtained K_{sv} value from the slope of F_0/F versus [Q] with interaction of ECT-AgNPs is 1.005×10^4 M^{-1} and ECT is 2.607×10^4 M^{-1} with $R^2 = 0.987$ and $R^2 = 0.982$. The resulting plot exhibits a good linearity. It indicates that either static or dynamic quenching plays a major role in the quenching process.

The possibility of static or dynamic quenching is verified by calculating bimolecular quenching rate constant (kq) using the following equation,

$$F_0 / F = 1 + K_q \tau_0 [Q] \quad (2)$$

τ_0 is the life time of the BSA fluorophores which is about 6×10^{-8}. From the obtained value of K_{SV}, the calculated Kq are found to be 1.676×10^{11} M^{-1} s^{-1} and 4.345×10^{11} M^{-1} s^{-1} for BSA with ECT and ECT-AgNPs respectively.

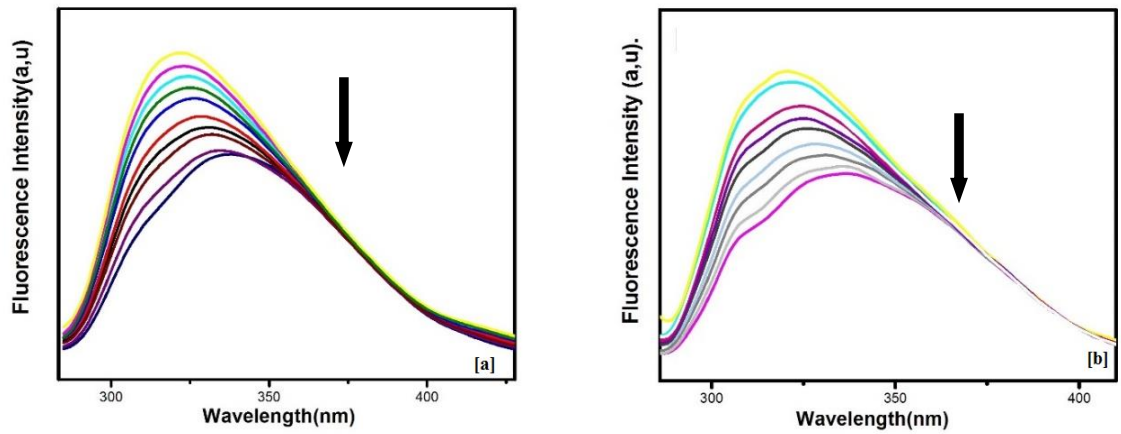

Fig 4.4 Variation in the intrinsic fluorescence of BSA on interaction with (a) ECT (b) AgNPs with ECT

The above values are higher than the maximum value possible for diffusion limited quenching ($10\times^{-10}$ M^{-1} s^{-1}). This suggests that there is a specific interaction that occurs between BSA and ECT and ECT-AgNPs. It also shows that ECT and ECT-AgNPs quenches BSA intrinsic fluorescence through the static quenching mechanism, which promotes the creation of ground state complexes between BSA and ECT, BSA and ECT-AgNPs. This high magnitude of observed K_q can be attributed to the process of complex formation via hydrophobic and hydrogen bond interaction between hydroxyl groups of ECT and ECT-AgNPs and aromatic residues of BSA .The obtained bimolecular quenching constants for these compounds are on the order of 10^{11}L mol^{-1} s^{-1}, which is 10-fold higher than the maximum value possible for diffusion controlled quenching (i.e., 2.0×10^{-10} mol^{-1} s^{-1}). This observation suggests that there is a specific interaction between the proteins and complexes and the probable quenching mechanism was not initiated by dynamic quenching but by a static one.

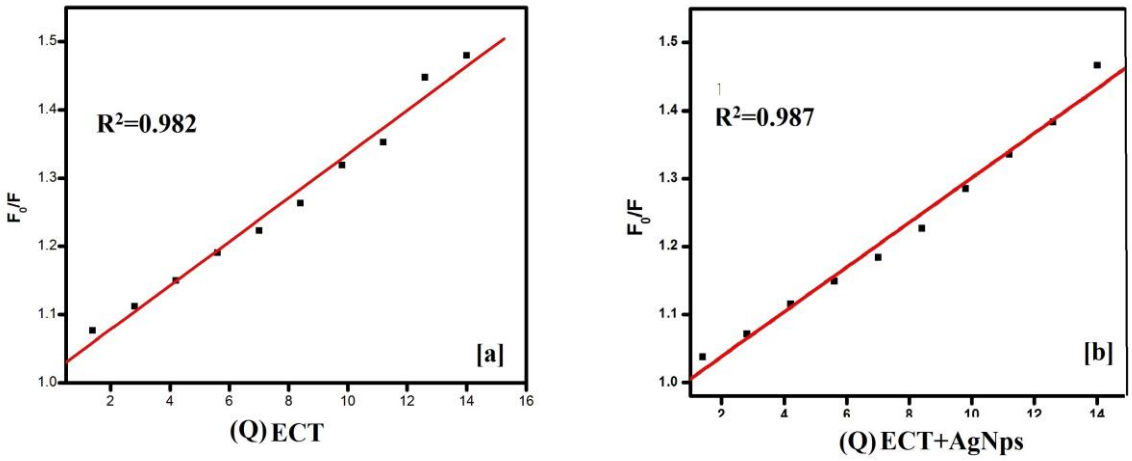

Fig.4.5 Stern-Volmer plot for BSA with (a) ECT (b) ECT-AgNPs

4.3.3. Binding Parameters of BSA-ECT and BSA-ECT-AgNPs Complexes.

The binding parameters are important to study pharmacodynamics and pharmacokinetics. When a small molecule binds independently to a set of homologous sites on a large molecule, the convergence between the free molecule and the binding molecule is calculated by the following equation

$$\log_{10}\left[\frac{F_0-F}{F}\right] = \log_{10} K_a + n \log_{10}[Q] \qquad (3)$$

where, K_a is the apparent binding constant to a site, and n is the number of binding sites per BSA. By the linear plot of $\log_{10}[(F_0\text{-}F)/F]$ versus $\log_{10}[Q]$, n and K_a can be obtained from the intercept and slope of the plot for the interaction of BSA with ECT-AgNPs and ECT, as shown in Fig 4.6 respectively. For positive cooperativity, $n > 1$, which signifies that the adsorption of a BSA molecule on the nanoparticle surface enhances the attachment of other protein units to the same surface. In contrast, for negative cooperativity, $n < 1$, which means that when additional BSA are adsorbed to the surface, the binding affinity of the BSA is gradually decreases and $n = 1$ reflects non-cooperative interactions where the resulting binding of BSA is independent of the proteins already bound to the surface [41]. The binding constant and the number of binding sites are found to be $K_a = 4.897\times10^4$ L mol^{-1}, n = 1.03 for ECT-AgNPs and for ECT, $K_a = 2.483\times10^4$ L mol^{-1}, n = 0.99(n<1). This indicates that binding of ECT/ECT-AgNPs occurs at only one site of BSA with 1:1.

The spontaneity of the association of the AgNPs with BSA was evaluated using the following Gibb's equation

$$\Delta G = -2.303\ 67\ RT\ \log K_a \qquad (4)$$

The obtained Gibb's free energy for ECT-AgNPs with BSA is -27.449 kJ/mol and for ECT is -25.620 kJ/mol. The negative ΔG values for the complexation of the ECT-AgNPs with BSA indicate the spontaneity of the interaction process.[23]

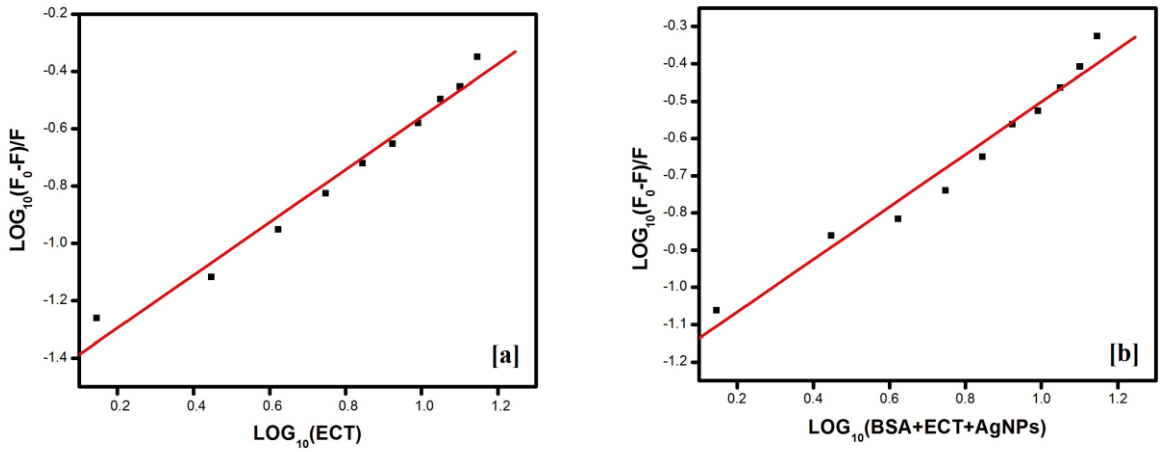

Fig 4.6 Stern-Volmer plot for $\log_{10}$ [(F_O-F)/F] versus [a] ECT and [b]ECT-AgNPs

Table 4.6 Binding parameters of BSA-ECT and BSA-ECT-AgNPs

Complex	K_{sv} (10^4 ,M^{-1})	K_q (10^{11}, M^{-1} s^{-1})	K_a (10^4, M^{-1})	n	ΔG (kJ/mol)
BSA-ECT	1.005	1.676	2.483	0.99	-25.620
BSA+ECT-AgNPs	2.607	4.345	4.897	1.03	-27.449

4.5 Antibacterial Activity.

The nano dimension of AgNPs means that they have a higher surface-to-volume ratio relative to their bulk counterparts. This property of AgNPs facilitates their interaction with bacterial surfaces, which enhances the anti-bacterial propensity of AgNPs. By monitoring the zone of inhibition, the well diffusion method was used to investigate the antibacterial impact of AgNPs against *Staphylococcus aureus* (*S.aureus*) *(Gram-positive) and Pseudomonas aeruginosa* (*P.aeruginosa*) *(Gram-negative)* bacterial strains which is shown in Fig 4.7. The diameter of the inhibition zones is measured and tabulated in Table 4.2. The release of Ag^+ ions from AgNPs to bacterial cells is responsible for the improved bactericidal impact of AgNPs. The zone of inhibition of BSA-ECT-AgNPs is 26mm, BSA-ECT mm is 20mm, ECT-AgNPs is 20mm and ECT is 17mm against *S.aureus* and against *P.aeruginosa* the BSA-ECT-AgNPs is 24mm, BSA-ECTmm is 20mm, ECT-AgNPs is 19mm and ECT is 17mm. The maximum zone of inhibition of 26 mm was found at BSA-ECT-AgNPs against *S. aureus* and 24 mm against *P.ae*ruginosa . From Table 4.2 and Fig. 4.7, it can be seen that BSA-Ct-AgNPs showed enhanced anti-bacterial effects (growth inhibition is confirmed by the clear inhibitory zones) against both *S.aureus* and *P.aeruginosa* as compared with samples BSA-ECT, ECT-AgNPs and ECT as depicted in Fig. 4.7

Table 4.2 Zone of inhibition of the Bacterial Strains.

Compound	***Staphylococcus aureus* (mm)**	***Pseudomonas aeruginosa* (mm)**
BSA-ECT-AgNPs	26	24
BSA-ECT	20	20
ECT-AgNPs	20	19
ECT	17	17

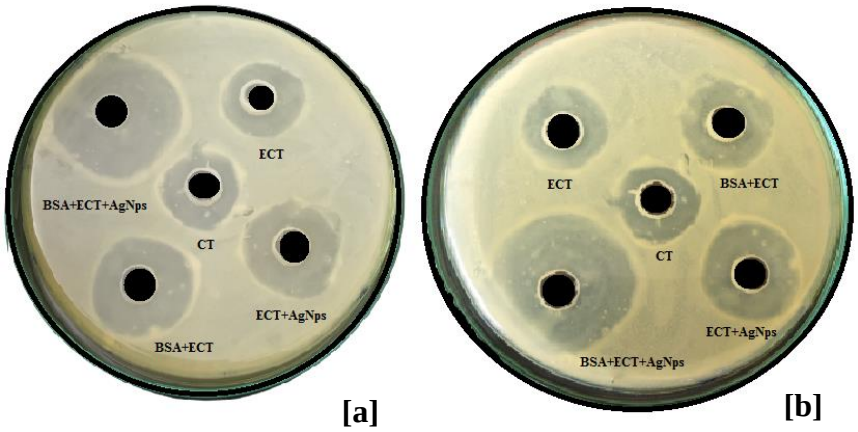

Fig 4.7 - Antibacterial efficiency of BSA-ECtAgNPs, ECT-AgNPs, BSA-ECT and ECT against (a) *Staphylococcus aureus* (b) *Pseudomonas aeruginosa*

4.7 MOLECULAR DOCKING.

Molecular docking is an effective in silico method implemented to identify the protein-ligand binding site and obtain the binding affinity of the binding site. The structure of BSA is made up of three homologous α-helical domains I, II and III, each domain is constituted by two subdomains A and B. The ligand binds to BSA at major binding site of sudlow site I which is found at Domain IA respectively. The blind docking confirmed that the binding site is identified in subdomain IA at sudlow site I for BSA and ECT and also BSA and ECT-AgNPs interaction. The molecular docking conformations of BSA –ECT and BSA-ECT-AgNPs with lowest binding energy are presented in the Fig.4.6.1 (a and b) respectively. The binding affinity of BSA-ECT has been found to be -7.0 kcal/mol and for BSA-ECT-AgNPs the binding affinity has been found to be -2.8 kcal/mol. During the interaction, the amino acid residues involved in the interaction of ECT at site I of BSA are Glu140, Arg185, Tyr160, Leu 122, Ile 181. And the amino acid residues involved in the interaction of ECT-AgNPs at site I of BSA were Leu24 and Lys20.

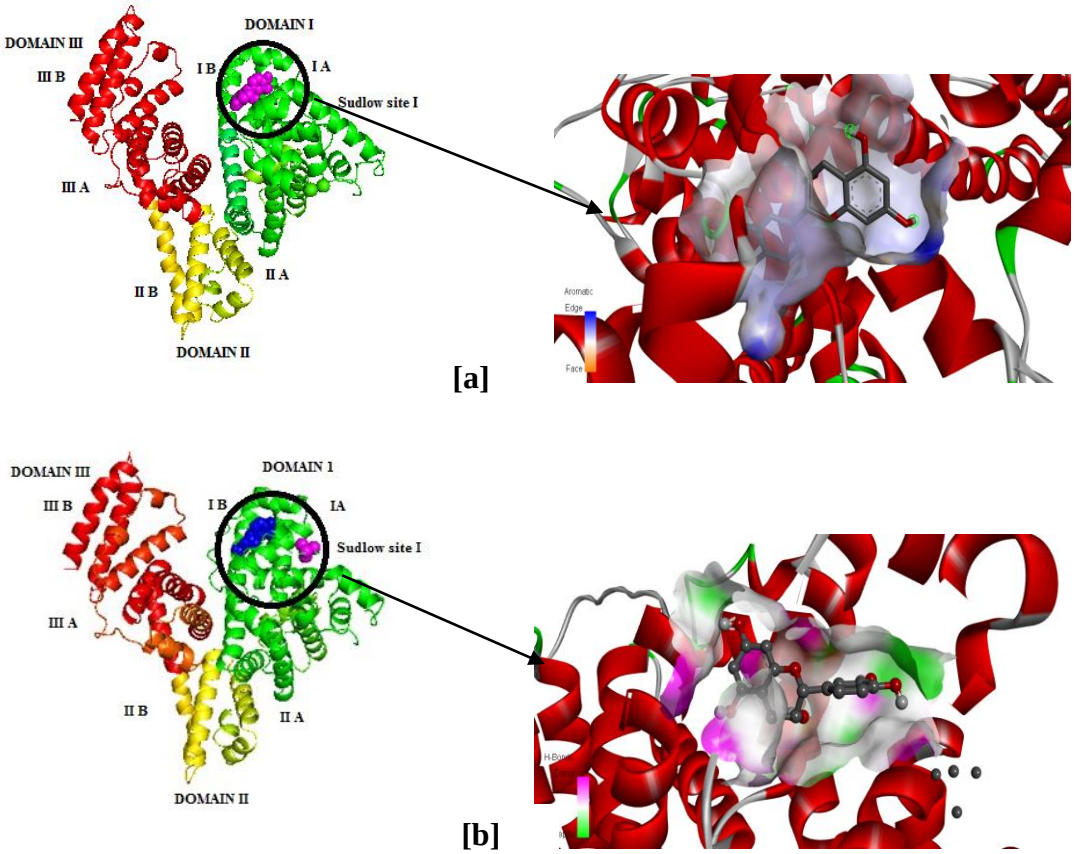

Fig 4.6.1 - The molecular docking conformation of (a) BSA-ECT and (b) BSA-ECT-AgNps complex with high binding affinity.

The binding of ECT with BSA and ECT-AgNPs with BSA protein occurs by hydrogen bond interaction through hydroxyl groups of ECT and polar residues of BSA, as well as hydrophobic interaction between ECT planar ring surfaces and non-polar residues of BSA. The interaction plot produced by Ligplots given in Fig. 5a and 5b. The hydrophobic interacting residues labelled in red arcs surrounded by ECT and BSA site I are Lys211, Thr231, Phe22, Val215, Gly 327, Leu330, Leu 326,Glu 353, Asp 323 shown in (Fig.4.6.2 a) similarly for ECT-AgNPs and BSA at sie I are Arg 185,Ile 141, Glu140, Leu 115, Tys137,Phe133,Lys 136.Leu122,Tyr 160 as shown in (Fig 4.6.2 b).

The structural stability of the biomolecular complexes is sustained by the formation of hydrogen bond. In the case of the BSA-ECT-AgNPs complex, one hydrogen bond is formed between ECT -AgNPs and the amino acid residue Ile181 with bond distance of 3.23 Å respectively (Fig. 4.6.2 b)[23].

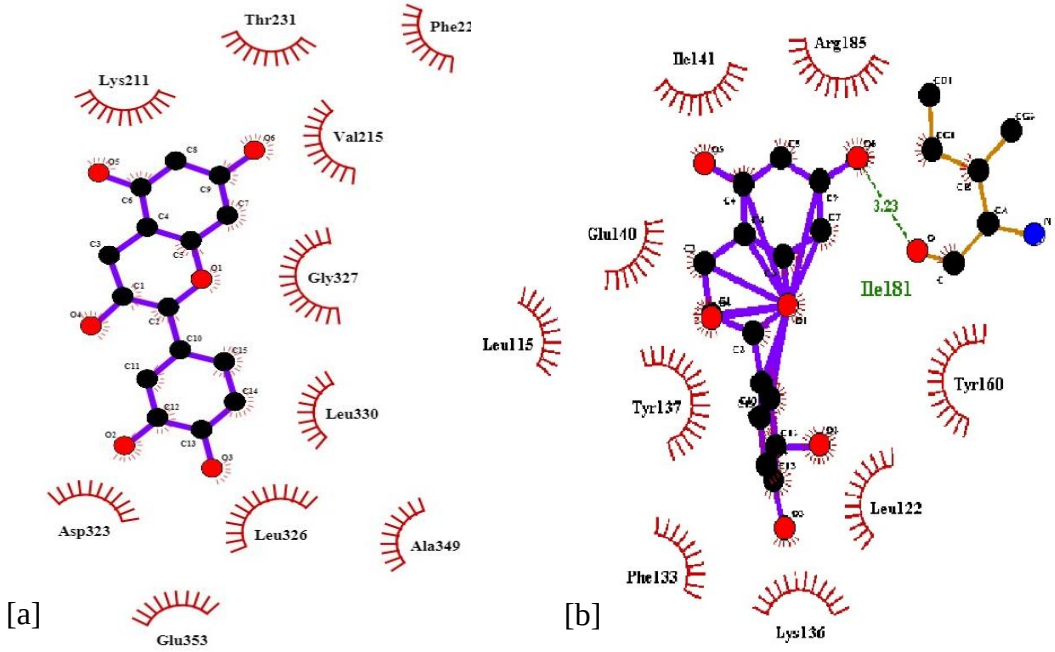

Fig 4.6.2 Two dimensional representations of ligplot of hydrophobic interaction residues of (a) BSA with ECT and (b)BSA-ECT+AgNps.

SUMMARY AND CONCLUSION

CHAPTER V
SUMMARY AND CONCLUSION

In this study the silver nanoparticle (AgNPs) was synthesized by (-) Epiatechin (ECT). The formation of AgNPs was observed by the colour change from colourless to pale yellow and it was confirmed by UV-Vis spectroscopy, TEM Analysis.TEM studies revealed that the spherical shaped nanoparticles were in the range of 20-60nm. The binding mechanism of the interaction of flavanols ECT and ECT-AgNPs with BSA protein has been investigated using spectroscopic techniques. According to fluorescence spectra, ECT/ECT-AgNPs interacts with BSA and quenches its intrinsic fluorescence via a static quenching mechanism and the values obtained for ECT/ECT-AgNPs $K_{SV=}$ 1.005×10^4 M^{-1} and 2.0671×10^4 M^{-1}, K_q= 1.676×10^{11} $M^{-1}s^{-1}$ and 4.345×10^{11} $M^{-1}s^{-1}$, K_a=4.4283×10^4 L mol^{-1} and 4.897×10^4 L mol^{-1}, n=0.9 and 1.03. This indicates that binding of ECT and ECT+AgNPs occurs at only one site of BSA with 1:1. The negative ΔG values for the complexation of ECT and ECT-AgNPs with BSA individually indicate the spontaneity of the interaction process and ECT exhibit analogous binding constant due to the similar functional groups. Molecular docking study confirms that the binding of ECT/ECT-AgNPs occurs in the sudlow site of I with subdomain IA of BSA respectively. The synthesized AgNPs using ECT proved the enhanced antibacterial activity against *Staphylococcus aureus* and *Pseudomonas aeruginosa.*

REFERENCES

REFERENCES.

[1] Tamara Topală; Andreea Bodoki; Luminiţa Oprean; Radu Oprean, Bovine serum albumin interactions with metal complexes. Clujul Medical, 87(4),(2014).

[2] Liu H, Shi X, Xu M, Li Z, Huang J, Bai D. Transition metal complexes of 2, 6-di ((phenazonyl-4-imino)methyl)-4-methylphenol structure and biological evaluation. Eur J Med Chem. 46(5),1638–1647, (2011).

[3] Sathyadevi P, Krishnamoorthy P, Jayanthi E, Butorac RR, Cowley AH, Dharmaraj N. Studies on the effect of metal ions of hydrazone complexes on interaction with nucleic acids, bovine serum albumin and antioxidant properties. Inorganica Chimica Acta. 83–96 (2012).

[4] Karolina A. Majorek; Przemyslaw J. Porebski; Arjun Dayal; Matthew D. Zimmerman; Kamila Jablonska; Alan J. Stewart; Maksymilian Chruszcz; Wladek Minor. Structural and immunologic characterization of Bovine,Horse and Rabbit serum albumins,(3-4),(2012).

[5] Philippe Rondeau, Emmanuel Bourdon, The Glycation of Albumin: Structural and Functional Impacts; Journal of Biochimie,93(4),645- 658, (2011).

[6] Topală, Tamara; Bodoki, Andreea; Oprean, Luminiţa; Oprean, Radu. Bovine serum albumin interactions with metal complexes. Clujul Medical, 87(4),(2014).

[7] In Meyler's Side Effects of Drugs (Sixteenth Edition), 2016.

[8] Reddy, Michael K.. "amino acid". Encyclopedia Britannica,(2020).

[9] Trumbo P, Schlicker S, Yates AA, Poos M; Food and Nutrition Board of the Institute of Medicine, The National Academies. Dietary reference intakes for energy, carbohydrate, fiber, fat, fatty acids, cholesterol, protein and amino acids,102(11),1621-1630.(2002).

[10] Tsao, Rong,Chemistry and Biochemistry of Dietary Polyphenols. Nutrients,2(12),1231–1246. (2010).

[11] Maarit J Rein, Mathieu Renouf, Cristina Cruz-Hernandez, Lucas Actis-Goretta, Sagar K Thakkar; Marcia da Silva Pinto, Bioavailability of Bioactive Food Compounds: A Challenging Journey to Bioefficacy. British Journal of Clinical Pharmacology,75(3),(2012).

[12] Kumar, Shashank; Pandey, Abhay K.. Chemistry and Biological Activities of Flavonoids: An Overview. The Scientific World Journal,(1-16),(2013).

[13] Falcone Ferreyra, María L, Rius, Sebastián P, Casati, Paula. Flavonoids: biosynthesis,biological functions, and biotechnological applications. Frontiers in Plant Science, 3(222),(2012).

[14] Han X., Shen T. and Lou H. Dietary polyphenols and their biological significance. Int J Mol Sci,8(9),950-988.(2007).

[15] Panche A.N., Diwan A.D., and Chandra S.R. Flavonoids: an overview. J Nutr Sci, 47,(2016).

[16] Mariel Calderón-Oliver, Edith Ponce-Alquicira, in Natural and Artificial Flavoring Agents and Food Dyes, 2018.

[17] Lide, D. R."Magnetic susceptibility of the elements and inorganic compounds". CRC Handbook of Chemistry and Physics,(95),(2005).

[18] Cassano D, Mapanao AK, Summa M, Vlamidis Y, Giannone G, Santi M. Biosafety and Biokinetics of Noble Metals: The Impact of Their Chemical Nature". ACS Applied Bio Materials. 2(10),4464–4470. (2019).

[19] Xi-Feng Zhang, Zhi-Guo Liu,; Wei Shen ; Sangiliyandi Gurunathan,. Silver Nanoparticles: Synthesis, Characterization, Properties, Applications, and Therapeutic Approaches. International Journal of Molecular Sciences, 17(9),(2016).

[20] Junwei Zhao, Qian Zhang, Wenquan Liu, Guiye Shan, Xin Wang. Biocompatible BSA-Ag2S nanoparticles for photothermal therapy of cancer. (2022).

[21] Sourav Das , Leader Langbang , Mahabul Haque , Vinay Kumar Belwal , Kripamoy Aguan , Atanu Singha Roy S. Biocompatible silver nanoparticles: An investigation into their protein binding efficacies, anti-bacterial effects and cell cytotoxicity studies. Journal of Pharmaceutical Analysis,(4),422-434,(2020).

[22] Jules-blaise mabou leuna, Martin pengou, Francis merlin melataguia tchieno, Sergeot delor kungo sop , Achille nassi, Charles pe´guy nanseu-njiki and Emmanuel ngameni. Electrochemical and spectroscopic studies of the interaction of (+)- epicatechin with bovine serum albumin. J.Chem. Sci,133(44) (2021)

[23] Anitha S, Saranya V, Shankar R, Sasirekha V. Structural exploration of interactions of (+) catechin and (−) epicatechin with bovine serum albumin:

Insights from molecular dynamics and spectroscopic methods.Journal of Molecular Liquids. (2021)

[24] Hashemnia, Sedigheh; Zarei, Hajar; Mokhtari, Zaynab; Mokhtari, Mohammad Hossein. An investigation of the effect of PVP-coated silver nanoparticles on the interaction between clonazepam and bovine serum albumin based on molecular dynamics simulations and molecular docking. Journal of Molecular Liquids,323,(2021).

[25] Farhat Ikram, Amtul Qayoom, Naheed Ikram and Muhammad Raza shah. Synergetic effect of epicatechin coated silver nanoparticles on antimicrobial activity of gentamicin against aspergillus niger. (2017).

[26] Daniel J. Boehmler, Zachary J. O'Dell, Christopher Chung, and Kathryn R. Bovine Serum Albumin Enhances Silver Nanoparticle Dissolution Kinetics in a Size- and Concentration-Dependent Manner.36(4),1053-1061,(2020).

[27] Jie Yang, Xiang-rong Liu, Ming-kun Yu,Wen-bo Yang, Zai- wen Yang,Shun-sheng Zhao. Co and Cu complexes with 2-acetylpyridine-4-hydroxy phenylacetyl acylhydrazone: Synthesis, crystal structures, CT-DNA/BSA binding behaviors, antibacterial activities and molecular docking studiesPolyhedron, (2020).

[28] Md Abrar Siddiquee, Mehraj ud din Parray, Syed Hassan Mehdi, KhalidAhmed Alzahrani, Abdulmohsen Ali Alshehri, Maqsood Ahmad Malik, Rajan Patel. Green synthesis of silver nanoparticles from Delonix regia leaf extracts: In-vitro cytotoxicity and interaction studies with bovine serum albumin. (2019).

[29] Junling Wang, Jianguo Zhao, Guibin Ma. Extremely concentrated silver nanoparticles stabilized in aqueous solution by Bovine Serum Albumin (BSA). Nano-Structures & Nano-Objects, 19,(2019).

[30] Farhat Ikram, Amtul Qayoom, Zara Aslam, Muhammad Raza Shah, Epicatechin coated silver nanoparticles as highly selective nanosensor for the detection of Pb2+in environmental samples. Journal of Molecular Liquids**,** (2018).

[31] Xiangyu Xu, Xuyan Mao; Yunfei Wang; Dandan Li; Zhongyu Du, Weihua Wu,Liang Jiang, Jie Yang, Jianjun Li, Study on the interaction of graphene oxide-silver nanocomposites with bovine serum albumin and the formation of nanoparticle-protein corona. International Journal of Biological Macromolecules, 116,492-501,(2018).

[32] Farhat Ikram, Amtul Qayoom, Muhammad Raza Shah,. Synthesis of Epicatechin Coated Silver Nanoparticles for Selective Recognition of Gentamicin. Sensors and Actuators B: Chemical, 257, 897-905 (2017).

[33] Jang Hoon Kim, Hyo Young Kim, Seo Young Yang,; Jin-Baek Kim; Jin, Chang Hyun,Young Ho Kim,. Inhibitory activity of (-)-epicatechin-3,5- O - digallate on α-glucosidase and in silico analysis. International Journal of Biological Macromolecules, (2017).

[34] Gebregeorgis, A., Bhan, C, Wilson, O, & Raghavan D.Characterization of Silver/Bovine Serum Albumin (Ag/BSA) nanoparticles structure: Morphological, compositional, and interaction studies. Journal of Colloid and Interface Science,1,31–41, (2013).

[35] Zhai Min; Wu HaiLong; Zhang ShuRong; Zhang XiHua; Sun YanMei; Yu RuQin. Interaction of epicatechin with bovine serum albumin using fluorescence quenching combined with chemometrics. Science China Chemistry, 748–754, (2014).

[36] Thomas V. Mathew; Sunny Kuriakose. Studies on the antimicrobial properties of colloidal silver nanoparticles stabilized by bovine serum albumin. 1,(101),(2013)

[37] Goutam Kumar Chandra, Debi Ranjan Tripathy, Dasgupta, Roy Swagata, Anushree . Interaction of (-)-Epigallocatechin Gallate with Lysozyme-Conjugated Silver Nanoparticles. Applied Spectroscopy, 744-749,(2012).

[38] Mihaela Skrt, Evgen Benedik ,rtomir Podlipnik , Natasa Poklar Ulrih. Interactions of different polyphenols with bovine serum albumin using fluorescence quenching and molecular docking. 135(4),2418-2424,(2014)

[39] Richard A. Frazier; Athina Papadopoulou; Rebecca J. Green. Isothermal titration calorimetry study of epicatechin binding to serum albumin,41(5),1602–1605, (2006).

[40] Behera S.; Behura R.; Mohanty M.; Dinda R.; Mohanty P.; Verma Anil K.; Sahoo, Suban K.; Jali B.R. Spectroscopic, cytotoxicity and molecular docking studies on the interaction between 2,4-dinitrophenylhydrazine derived Schiff bases with bovine serum albumin. Sensors International. 1, (2020).

[41] Principle-working-and-applications-of-UV-spectroscopy, Indiastudychannel.

[42] D.R. Baer, S. Thevuthasan, Characterization of Thin Films and Coatings. In Handbook of Deposition Technologies for Films and Coatings (Third Edition).(2010)

[43] Gfroerer T., H. Photoluminescence in Analysis of Surfaces and Interfaces**.** In Encyclopaedia of Analytical Chemistry; Meyers, R. A., Ed.; John Wiley and Sons Ltd.: Chichester,10815-10837,(2000).

[44] David B. Williams and C. Barry Carter, Electron microscopy of thin crystals, Peter Hirsch.(1965).

[45] Ahmad Anees, Syed; Sabya Sachi Das; Ayesha Khatoon; Tahir Ansari, Mohd Mohammed Afzal;Md Saquib Hasnain; Amit Kumar Nayak. Bactericidal activity of silver nanoparticles: A mechanistic review. Materials Science for Energy Technologies.3,756-769,(2020).

[46] Mounyr Balouiri; Moulay Sadiki,; Saad Koraichi Ibnsouda. Methods for in vitro evaluating antimicrobial activity: A review. Journal of Pharmaceutical Analysis,71-79,(2015).

[47] Xuetuan Wei; Mingfang Luo; Wei Li; Liangrong Yang; Xiangfeng Liang; Lin Xu; Peng Kong; Huizhou Liu. Synthesis of silver nanoparticles by solar irradiation of cell-free Bacillus amyloliquefaciens extracts and AgNO3. 103(1),273–278. (2012).

[48] Prakash Periakaruppan, P.Gnanaprakasam, Roham Emmanual, Arokiaraj Selvaraj, Green synthesis of silver nanoparticles from leaf extracts of Mimusops. Colloids & Surface B: Biointerfaces,(2012).

[49] Gloria E. Campillo, Ederley Vélez, Gladis Morales, César Hincapié , Jaime Osorio, Oscar Arnache , José Ignacio Uribe, Franklin Jaramillo, Synthesis of Silver nanoparticles (AgNPs) with Antibacterial Activity.(2017).

[50] X. Li, Y. Hao, Probing the binding of (+) -catechin to bovine serum albumin by isothermal titration calorimetry and spectroscopic techniques, J. Mol. Struct. 1091,(2015)

[51] Bhogale, N. Patel, J. Mariam, P. Dongre, A. Miotello, D. Kothari, Comprehensive studies on the interaction of copper nanoparticles with bovine serum albumin using various spectroscopies, Colloids and Surfaces B: Biointerfaces, 113,276-84,(2014).